

# Forces and pressures in adsorbing partially directed walks

**E.J. Janse van Rensburg<sup>1†</sup> and T. Prellberg<sup>2‡</sup>**

<sup>1</sup>Department of Mathematics and Statistics, York University, Toronto, Ontario M3J 1P3, Canada

<sup>2</sup>School of Mathematical Sciences, Queen Mary, University of London, Mile End Road, London E1 4NS, United Kingdom

**Abstract.** Polymers in confined spaces lose conformational entropy. This induces a net repulsive entropic force on the walls of the confining space. A model for this phenomenon is a lattice walk between confining walls, and in this paper a model of an adsorbing partially directed walk is used. The walk is placed in a half square lattice  $\mathbb{L}_+^2$  with boundary  $\partial\mathbb{L}_+^2$ , and confined between two vertical parallel walls, which are vertical lines in the lattice, a distance  $w$  apart. The free energy of the walk is determined, as a function of  $w$ , for walks with endpoints in the confining walls and adsorbing in  $\partial\mathbb{L}_+^2$ . This gives the entropic force on the confining walls as a function of  $w$ . It is shown that there are zero force points in this model and the locations of these points are determined, in some cases exactly, and in other cases asymptotically.

AMS classification scheme numbers: 82B41, 82B23

† rensburg@yorku.ca

‡ t.prellberg@qmul.ac.uk

## 1. Introduction

A linear polymer in a good solvent placed near a geometric obstacle (such as a hard wall) loses conformational entropy. This loss of entropy induces a net force on the obstacle [24], and if the polymer can move freely, then it will tend to move away from the obstacle. The induced force is repulsive, and the polymer exerts an average net pressure on the wall. These entropic pressures have been seen in experiments [2, 6, 12] and have been modelled numerically (see for example reference [21]).

A similar situation is seen when a polymer is placed in a confined space; the loss in conformational entropy induces a net repulsive force on the walls of the confined space. For example, a polymer between two colloidal particles loses entropy as the particles approach one another; this induces a net repulsive force between the two particles. The repulsion between particles is the mechanism underlying the stabilization of a colloid by a polymer [25]. This phenomenon was examined numerically using a self-avoiding walk model of a polymer confined between two hard walls [8]. A self-interaction self-avoiding walk model of polymer pulled at its endpoints was similarly considered in reference [13, 21]. See references [27, 30, 31] for more results.

In this paper a two dimensional partially directed walk model is used to model the entropic forces induced by an adsorbing polymer between confining walls. In addition, the entropic pressure of an adsorbing polymer on the adsorbing wall will be examined as well. Similar models were examined in reference [17], using directed path models to model the pressure of a directed path on the adsorbing boundary. Related work on the entropic pressure near knotted lattice ring polymers was reported in reference [14], which built on the results in references [11, 19].

In this paper we continue the study of entropic pressure near lattice polymers by using a partially directed walk model in the square lattice. Directed path models were examined in reference [17], where the entropic pressure near directed paths and staircase polygons models (of a grafted linear polymer) was calculated. In particular, for a directed path of length  $n$  from the origin in the positive half-lattice, the pressure on the  $x$ -axis a distance proportional to  $an$  from the origin is given by

$$P_n(a) = -\frac{2\sqrt{2}}{\sqrt{\pi n^3 a^3(1-a)}} + O(n^{-5/2}). \quad (1)$$

This, in particular, shows that

$$\lim_{n \rightarrow \infty} n^{3/2} P_n(a) = -\frac{2\sqrt{2}}{\sqrt{\pi a^3(1-a)}} \quad (2)$$

as  $n \rightarrow \infty$ .

Partially directed walk models of polymers were introduced in references [7, 29], and have been widely used as models of polymer entropy; see for example references [4, 5, 10]. The generating function of adsorbing partially directed walks has been computed in several models using the Temperley method [28], and in this paper we will follow a similar approach to that of reference [26].

Let  $\mathbb{Z}^2$  be the *square grid* with standard basis  $\{\vec{e}_1, \vec{e}_2\}$ . A point or *vertex*  $\vec{x} \in \mathbb{Z}^2$  is a vector with Cartesian coordinates  $(\vec{x}(1), \vec{x}(2))$ . Two points  $\vec{x}, \vec{y} \in \mathbb{Z}^2$  are *adjacent* in  $\mathbb{Z}^2$  if  $\|\vec{x} - \vec{y}\|_2 = 1$ . The *edge*  $\langle \vec{x} \sim \vec{y} \rangle$  is a unit length line segment between adjacent

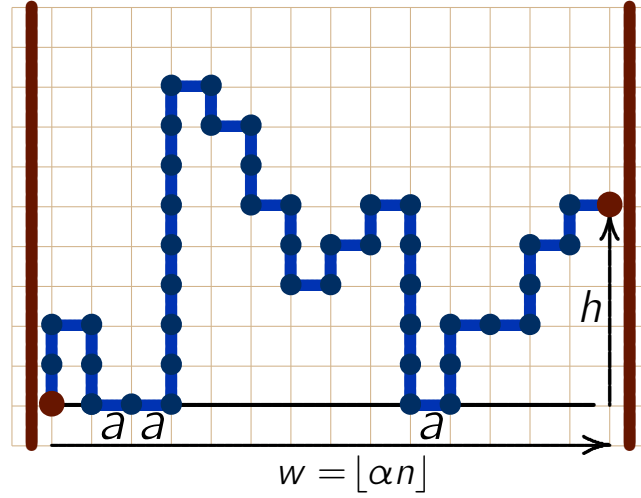


Figure 1: A partially directed walk from the origin in  $\mathbb{L}_+^2$  of width  $w$  and endpoint at height  $h$ . The walk is weighted by the activity  $a$  conjugate to the number of edge-visits in  $\partial\mathbb{L}_+^2$  and its endpoints are tethered to two vertical walls a distance  $w$  apart which bounds a confining space (vertical slit of width  $w$ ) containing the walk. If  $h = 0$  then this is an *adsorbing bargraph path* from the origin in  $\mathbb{L}_+^2$ .

points (or vertices)  $\vec{x}$  and  $\vec{y}$  in  $\mathbb{Z}^2$ . The *square lattice*  $\mathbb{L}^2$  is the set of all edges between adjacent vertices of  $\mathbb{Z}^2$ , defined by

$$\mathbb{L}^2 = \{ \langle \vec{x} \sim \vec{y} \rangle \mid \vec{x}, \vec{y} \in \mathbb{Z}^2 \text{ and } \|\vec{x} - \vec{y}\|_2 = 1 \}. \quad (3)$$

The *positive square lattice* is given by

$$\mathbb{L}_+^2 = \{ \langle \vec{x} \sim \vec{y} \rangle \in \mathbb{L}^2 \mid \vec{x}(2) \geq 0 \text{ and } \vec{y}(2) \geq 0 \}. \quad (4)$$

The *boundary* of  $\mathbb{L}_+^2$  is given by

$$\partial\mathbb{L}_+^2 = \{ \langle \vec{x} \sim \vec{y} \rangle \in \mathbb{L}_+^2 \mid \vec{x}(2) = 0 \text{ and } \vec{y}(2) = 0 \} \quad (5)$$

and every edge in  $\partial\mathbb{L}_+^2$  is parallel to  $\vec{e}_1$  and normal to  $\vec{e}_2$ .

A *directed edge* is a directed unit length line segment from a vertex  $\vec{x}$  to a vertex  $\vec{y}$  in  $\mathbb{Z}^2$ . It is denoted by  $\langle \vec{x} \rightsquigarrow \vec{y} \rangle$ . A directed edge  $\langle \vec{x} \rightsquigarrow \vec{y} \rangle$  is in the East direction if  $\vec{x}(1)+1 = \vec{y}(1)$  and  $\vec{x}(2) = \vec{y}(2)$ , it is in the South direction if  $\vec{x}(1) = \vec{y}(1)$  and  $\vec{x}(2)-1 = \vec{y}(2)$  and it is in the North direction if  $\vec{x}(1) = \vec{y}(1)$  and  $\vec{x}(2)+1 = \vec{y}(2)$ .

A *partially directed walk*  $\omega$  in  $\mathbb{L}^2$  of length  $n$  is a sequence of  $n$  directed edges in the East (E), North (N) and South (S) directions, starting in  $\vec{0}$ , such that a directed edge in the N direction cannot immediately be followed by a directed edge in the S direction and vice versa. That is,  $\omega$  is a sequence of directed edges in the E, N and S directions  $\langle \vec{v}_0 \rightsquigarrow \vec{v}_1 \rangle, \langle \vec{v}_1 \rightsquigarrow \vec{v}_2 \rangle, \langle \vec{v}_2 \rightsquigarrow \vec{v}_3 \rangle, \dots, \langle \vec{v}_{n-1} \rightsquigarrow \vec{v}_n \rangle$  such that  $\vec{v}_0 = \vec{0}$  and all the  $\vec{v}_j$  are distinct (so that  $\omega$  is self-avoiding). The terminal or last vertex of  $\omega$  is  $\vec{v}_n$ .

If a directed walk from  $\vec{0}$  is in the positive square lattice  $\mathbb{L}_+^2$ , then it is a *positive partially directed walk*. A positive partially directed walk is illustrated in figure 1.

A partially directed walk from the origin in the positive half-lattice is illustrated in figure 1. Edges in the walk which are in the x-axis are weighted by the generating variable  $a$ . For large  $a$  the walk stays near the x-axis, so that this is a model of an *adsorbing partially directed walk*. In section 2 the generating function of walks of fixed width  $w$  is determined using the kernel method [3, 9]. In particular, we show that the generating

function of partially directed walks from the origin in the half-lattice, of width  $w$  with final vertex at height  $h$ , is

$$G_{wh}(a, y) = \sum_{s=0}^w \sum_{k=0}^w \sum_{i \geq 0} \frac{w+1-s}{w+i+1-s} \binom{h}{w-k-s} \binom{n-1}{i} \binom{w}{s-i} \frac{y^{h+2i}(a-1)^k}{(1-y^2)^s}. \quad (6)$$

The variable  $y$  generates vertical steps (and there are exactly  $w$  horizontal steps). This result can be used to extract the partition function of walks of length  $n$ , width  $w$  and last vertex at height  $h$  (see equation (37)).

In section 3 the entropic forces in the model are examined in the scaling limit, defined by putting  $w = \lfloor \alpha n \rfloor$  for walks of length  $n$ , and then taking  $n \rightarrow \infty$  in the model (see figure 1). This gives the limiting free energy  $F(\alpha)$  of the walk, which is computed for several cases. For example, for walks with  $h = 0$  and  $a = 1$ , the limiting free energy is given by

$$F_0(\alpha) = \alpha \log(2\alpha(1-\alpha)) - (\sqrt{C} + 2\alpha - 1) \log(\sqrt{C} + 2\alpha - 1) - (1 - \sqrt{C}) \log(1 - \sqrt{C}) + \frac{1}{2} \sqrt{C} \log\left(\frac{C+\alpha}{C-\alpha}\right), \quad (7)$$

where  $C = 2\alpha^2 - 2\alpha + 1$ . The derivative of this expression to  $\alpha$  gives the limiting force

$$\mathcal{F}_0(\alpha) = \frac{d}{d\alpha} F_0(\alpha) = \log\left(\frac{2\alpha(1-\alpha)}{(C+2\alpha-1)^2}\right) + \frac{C^2-2\alpha}{2C} \log\left(\frac{(C-\alpha)(2\alpha+C-1)^2}{(C+\alpha)(1-C)^2}\right). \quad (8)$$

It follows directly from the above that  $\mathcal{F}_0(\alpha) = -\mathcal{F}_0(1-\alpha)$  (so that  $\mathcal{F}_0(\frac{1}{2}) = 0$ ). That is, the limiting force vanishes (in the limit) when the confining walls are a distance  $w = \lfloor \frac{1}{2}n \rfloor$  apart. This is the *zero force point* in the model, and it is located in this model when the walk is extended one-half of its length along the adsorbing line (or when one-half of the edges (steps) in the walk is in the horizontal direction). The limiting force curve  $\mathcal{F}_0(\alpha)$  is also symmetric on reflection through the point  $(\frac{1}{2}, 0)$  in the  $(\alpha, \mathcal{F}_0(\alpha))$ -plane. For small  $\alpha > 0$  the above shows that  $\mathcal{F}_0(\alpha) \sim |\log \alpha|$  (see equation (65)).

In addition to the above, the asymptotic forces in other models are examined. These models include walks with a lifted endpoint, as well as walks which are adsorbing. In each case asymptotic expressions for the limiting forces are determined, and the location of the zero force point is determined.

In section 4 finite size asymptotics of the model is developed for the case that  $a = 1$ . The partition function simplifies to a single summation which may be approximated using a saddle-point method. We determine an asymptotic expression for the partition function, and we use this expression to determine the asymptotics for the repulsive force between vertical walls (see section 3). In particular, if the walk has length  $n$  and the confining walls are a distance  $\alpha n$  apart, then the asymptotic force has leading term asymptotics  $\mathcal{F}_n(\alpha) = -\frac{1}{\alpha} + (n - \frac{1}{2}) - n \log \alpha + O(n\alpha)$  as  $\alpha \searrow 0$ . For small values of  $\alpha$  the force is positive (repulsive).

In section 5 the model is examined numerically. This is done in particular to (1) verify the asymptotic results, and (2) to examine cases which we have not analysed in section 4. The approach is to determine forces and pressures in the models, using as starting point the expressions for the partition function and generating function determined in section 2. In the first instance the entropic forces exerted on two confining vertical walls by an adsorbing partially directed walk with endpoints tethered in the walls are determined

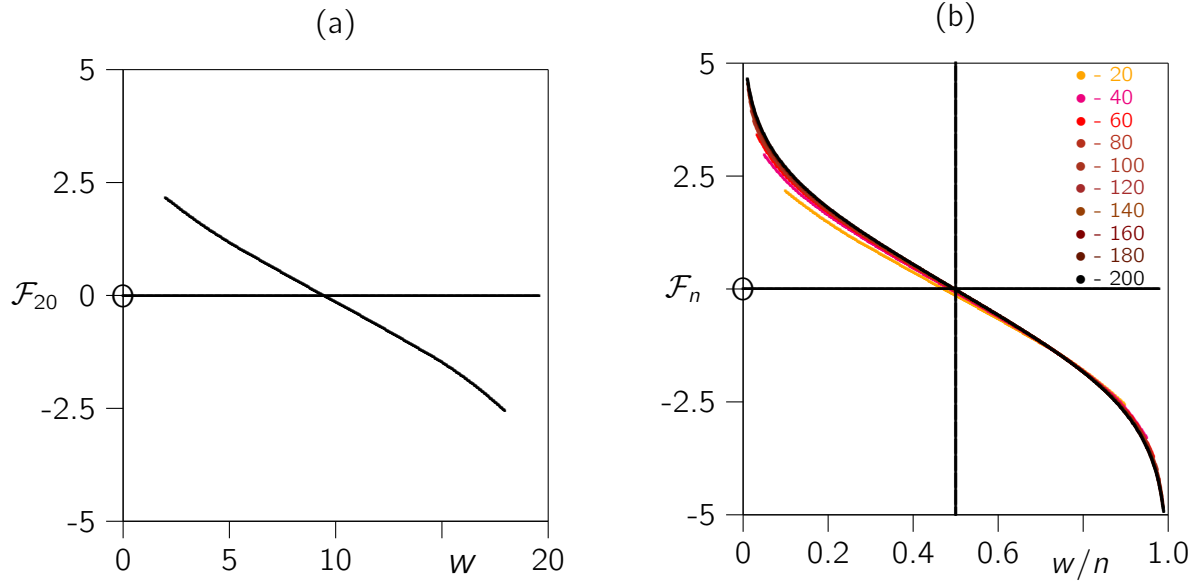


Figure 2: The entropic forces exerted by a partially directed walk confined between two vertical walls in  $\mathbb{L}_+^2$  (as shown in figure 1). (a) The force for walks of length  $n = 20$ , endpoint at height  $h = 0$ , and with  $a = 1$ , plotted as a function of  $w$ , the distance between the two walls (or equivalently, the width of the walk). For small values of  $w$  the force is positive (and therefore repulsive, pushing the walls away from one another). For large values of  $w$  the force is negative; this indicates an attractive force between the two walls. (b) Force curves for walks of lengths from  $n = 20$  to  $n = 200$ , for  $a = 1$  and  $h = 0$ , as a function of  $w$ . The horizontal length scale is normalised by  $n$  for each curve (so that  $w = \lfloor \alpha n \rfloor$  for  $0 \leq \alpha \leq 1$ ); this collapses the curves into a single force curve shown which tends to a limiting curve as  $n \rightarrow \infty$ . Notice that the forces vanish at approximately  $w = \frac{1}{2}n$ .

numerically (see figure 1). By rescaling the forces by the length of the walk, the data collapse to a single force curve which is repulsive when the confining walls are close together, and attractive when the confining walls are far apart. The typical situation is seen in figure 2 when  $a = 1$  and the height of the endpoint of the walk is  $h = 0$ . The force curves are modified when  $a > 1$ , generally becoming more repulsive as  $a$  increases (and taking the walk through its transition into its adsorbed phase).

Secondly, the pressure of the adsorbing partially directed walks on the adsorbing wall is examined. If the walk is tethered at the origin, then there is a large entropic pressure on the adsorbing wall close to the origin. This pressure decays quickly with distance from the origin. If both endpoints of the walk are confined to the adsorbing wall, then for walks of length  $n$  a secondary pressure peak is seen at a distance about  $\frac{1}{2}n$  from the origin – this peak is the result of the *other* endpoint of the walk (which exerts pressure in the vicinity of the point where the path returns to the adsorbing wall; see for example figure 15).

In section 6 we conclude the paper with a few final remarks.

## 2. Partially directed walks of width $w$

In this section the kernel method (see for example reference [3]) is used to determine  $G(\mu) \equiv G(x, y, \mu, a)$ , the generating function of partially directed walks from the origin

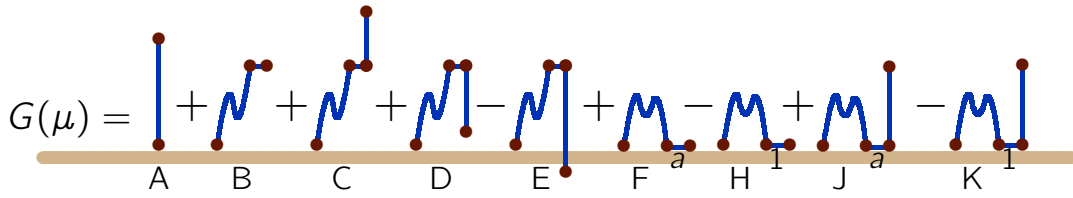


Figure 3: The generating function  $G(\mu)$  of partially directed walks from the origin in  $\mathbb{L}_+^2$ , with edge-visits weighted by  $a$  and height of endpoint weighted by  $\mu$ , may be classified as above. This classification gives a functional recurrence for  $G(\mu)$ . Each walk is either (A) a string of vertical edges (possibly of length 0), or (B) ends in a horizontal step at height  $h > 0$ , or (C) ends in a horizontal step followed by a non-empty sequence of steps in the up direction, or (D–E) ends in a horizontal step followed by a non-empty sequence steps in the South direction (downwards) which does not not step below  $\partial\mathbb{L}_+^2$ , or (F–H) ends in a horizontal step at height  $h = 0$  (subtracted out by H and added back in with weight  $a$  in F), or (J–K), ends in a horizontal edge at height  $h = 0$ , followed by a non-empty sequence of vertical edges, subtracted out in K, and then added back with weight  $a$  in J.

in  $\mathbb{L}_+^2$  with a collection of activities  $\{x, y, \mu, a\}$ , conjugate to length, height of endpoint, and number of edge-visits to  $\partial\mathbb{L}_+^2$ . Introduce the following generating variables:

- horizontal steps:  $x$ ;
- vertical steps:  $y$ ;
- edge-visits to the adsorbing boundary:  $a$ ;
- height of last vertex:  $\mu$ .

The variable  $\mu$  is the designated *catalytic variable*, and the generating function of this model is denoted by  $G(\mu)$  (the variables  $\{x, y, a\}$  compose a set of parameters or weights in the model). The generating function  $G(\mu)$  will be determined by first finding a functional recurrence for it, using the classification of partially directed walks illustrated in figure 3.

The contributions to the generating function in figure 3 are labeled by A through J, and some are subtracted out while most are added in. Accounting for horizontal and vertical steps, and for edge-visits, and height of the last vertex, the following generating functions are obtained for each of the terms:

$$\begin{aligned} A &= \frac{1}{1-y\mu}; & B &= x G(\mu); \\ C &= \frac{xy\mu}{1-y\mu} G(\mu); & D &= \frac{xy/\mu}{1-y/\mu} G(\mu); \\ E &= \frac{xy/\mu}{1-y/\mu} G(y); & F &= ax G(0); \\ H &= x G(0); & J &= \frac{axy\mu}{1-y\mu} G(0); \\ K &= \frac{xy\mu}{1-y\mu} G(0). \end{aligned}$$

Since  $G(\mu) = A+B+C+D-E+F-H+J-K$ , this gives the following functional recurrence for  $G(\mu)$ :

$$G(\mu) = \frac{1}{1-y\mu} + \left( x + \frac{xy\mu}{1-y\mu} + \frac{xy}{\mu-y} \right) G(\mu) + (a-1) \left( x + \frac{xy\mu}{1-y\mu} \right) G(0) - \frac{xy}{\mu-y} G(y). \quad (9)$$

Multiply through by  $(1-y\mu)(y-\mu)$  and simplify. The coefficient of  $G(\mu)$  is the *kernel*, given by

$$K(\mu) = \frac{y(1-(1-x+y^2+xy^2)\frac{\mu}{y}+\mu^2)}{(1-y\mu)(y-\mu)}. \quad (10)$$

The numerator of  $K(\mu)$  is a quadratic with roots  $\mu_0$  and  $\mu_1$  such that  $\mu_1 = 1/\mu_0$  and

$$\mu_0 = \frac{1}{2y} \left( 1-x + (1+x)y^2 + \sqrt{(1-x)^2 - 2(1+x^2)y^2 + (1+x)^2y^4} \right). \quad (11)$$

Notice that

$$K(\mu) = \frac{(1-\mu\mu_0)(1-\mu\mu_1)}{(1-\mu y)(1-\mu/y)} \quad (12)$$

so that  $K(0) = 1$ .

Series expansion of  $\mu_0$  and  $\mu_1$  shows that  $\mu_1$  counts a certain set of walks. Thus,  $\mu_1$  is a "physical root" and it will play a key role in determine  $G(\mu)$ . The substitution  $x = u(1-v)$  and  $y = \sqrt{v}$  in  $F = \frac{1}{xy}(\mu_1 - y) - 1$  gives

$$F = \frac{1}{2uv} \left( 1 - u(1+v) - \sqrt{1 - 2u(1+v) + u^2(1-v)^2} \right). \quad (13)$$

This may be expanded in  $u$  to obtain

$$F = u + (1+v)u^2 + (1+3v+v^2)u^3 + (1+6v+6v^2+v^3)u^4 \\ + (1+10v+20v^2+10v^3+v^4)u^5 + \dots \quad (14)$$

This is the series expansion of the Narayana generating function given by

$$N(u, v) = \sum_{s=1}^{\infty} \sum_{i=1}^s \frac{1}{s} \binom{s}{i} \binom{s}{i-1} v^{i-1} u^s. \quad (15)$$

That is,  $F \equiv N(u, v)$  and it follows that

$$\mu_1 = xy(N(x, y) + 1) + y. \quad (16)$$

The Narayana generating function has useful properties, which will be used later. In particular, powers of  $N(u, v)$  have nice expansions:

$$(N(u, v))^r = \sum_{s=1}^{\infty} \sum_{i=1}^N \frac{r}{s} \binom{s}{r+i-1} \binom{s}{i-1} v^{i-1} u^s. \quad (17)$$

Taking  $\mu = 0$  in equation (9) produces

$$G(y) = \frac{1}{x} ((1+x(1-a))G(0) - 1). \quad (18)$$

Using equation (12) and the above in the recurrence (9) gives

$$\frac{x(a-1)}{1-\mu y} G(0) + \frac{y}{\mu-y} (1+(xa-x-1)G(0)) + \frac{1}{1-\mu y} - \frac{(1-\mu\mu_0)(1-\mu\mu_1)}{(1-\mu y)(1-\mu/y)} G(\mu) = 0. \quad (19)$$

Substituting  $\mu = \mu_1$  gives  $G(0)$ :

$$G(0) = \frac{(1-y^2)\mu_1}{(x(1-y^2)(1-a) - y^2)\mu_1 + y}. \quad (20)$$

This is the generating function of walks ending in the adsorbing line (or with endpoint at height zero). Substituting this into equation (19) gives a solution for  $G(\mu)$ :

$$G(\mu) = \frac{(1-y^2)\mu_1}{(1-\mu\mu_1)((x(1-y^2)(1-a)-y^2)\mu_1+y)}. \quad (21)$$

Recall that  $K(\mu_1) = 0$ ; this is useful in simplifying  $G(\mu)$  to

$$G(\mu) = \frac{y-\mu_1}{x(1-\mu\mu_1)((a-1)\mu_1-ya)}. \quad (22)$$

Substituting  $x \rightarrow xt$ , and  $y \rightarrow yt$ , and then doing a series expansion in  $t$ , gives the series

$$1 + (xa+y\mu)t + (y^2\mu^2+xya\mu+x^2a^2+xy\mu)t^2 + (y^3\mu^3+xy^2a\mu^2+x^2ya^2\mu+x^3a^3+2xy^2\mu^2+x^2ya\mu+x^2y\mu+xy^2)t^3 + \dots, \quad (23)$$

of walks with  $t$  the length generating variable. Substituting  $\mu_1$  using the Narayana generating function above gives  $G(\mu)$  in terms of  $N(x, y)$ :

$$G(\mu) = \frac{N(x, y)+1}{(xa(N(x, y)+1) - xN(x, y) - x - 1)(xy\mu(N(x, y)+1) + y\mu - 1)}. \quad (24)$$

Introduce  $\lambda = x+xN(x, y)$  in equation (16). Then it follows that  $\mu_1 = y+y\lambda$ , and  $\lambda = \frac{1}{x}\mu_1 - 1$ . Define  $\sigma = a-1$ , then it follows that

$$G(\mu) = \frac{\lambda}{x(1-\sigma\lambda)(1-y\mu(\lambda+1))}. \quad (25)$$

By expanding this in a power series in  $y$ , the generating function of walks ending in a vertex at height  $h$  is

$$G_h(a, y) = \frac{\lambda y^h (1+\lambda)^h}{x(1-\sigma\lambda)}. \quad (26)$$

Substitute  $\lambda = x+xN(x, y)$  and suppress the arguments of  $N(x, y) \equiv N$  to simplify expressions. This gives

$$G_h(a, y) = \frac{(1+N)y^h(xN+x+1)^h}{1-(a-1)(x+xN)} \quad (27)$$

since  $\sigma = a-1$ , and in terms of the Narayana generating function  $N(x, y)$ . This completes the determination of the generating function  $G_h(a, y)$  of partially directed paths ending in a vertex at height  $h$ .

### 2.1. The generating function $G_{wh}(a, y)$ of partially directed walks of width $w$

The generating function of walks of width  $w$  and last vertex at height  $h$  can be extracted from  $G_h(a, y)$  in equation (27). The strategy is to expand  $G_h(a, y)$  in powers of  $\lambda = x+xN$ , and then to use equation (17) in order to simplify the expressions.

Expanding the denominator of  $G_h(a, y)$  in equation (26) in  $\lambda$  gives

$$G_h(a, y) = \frac{1}{x} \sum_{k=0}^{\infty} \sigma^k \lambda^{k+1} y^h (1+\lambda)^h. \quad (28)$$



Substituting  $\lambda = x(1+N)$  and simplifying leaves

$$G_h(a, y) = \sum_{k=0}^{\infty} \sigma^k x^k y^h (1+N)^{k+1} (1+x+xN)^h. \quad (29)$$

Let  $S(k)$  be the summand of  $G_h(\mu)$  above. By expanding the factors in  $S(k)$ , it follows that

$$S(k) = \sigma^k x^k y^h \sum_{j=0}^h \sum_{\ell=0}^{j+k+1} \binom{h}{j} \binom{k+j+1}{\ell} x^j N^\ell, \quad (30)$$

so  $G_h(a, y) = \sum_{k=0}^{\infty} S(k)$ . Reverse the order of the summations and allow  $\ell$  to run to  $\infty$  to simplify the expression. This gives

$$S(k) = \sigma^k x^k y^h \sum_{\ell=0}^{\infty} \sum_{j=0}^h \binom{h}{j} \binom{k+j+1}{\ell} x^j N^\ell. \quad (31)$$

This introduces powers of Narayana numbers which is replaced by using equation (17). Simplifying the resulting expression gives the following for  $S(k)$ :

$$S(k) = y^h x^k \sigma^k \sum_{\ell=0}^{\infty} \sum_{j=0}^h \binom{h}{j} \binom{k+j+1}{\ell} x^j \times \left[ \sum_{s=1}^{\infty} \sum_{i=1}^s \frac{\ell}{s} \binom{s}{i+\ell-1} \binom{s}{i-1} \left( \frac{x}{1-y^2} \right)^s y^{2i-2} \right]. \quad (32)$$

The powers of  $x$  in the summand is  $w = k+j+s$ . This is also the number of horizontal steps, and so is the horizontal width  $w$  of the walk. Extract the coefficient of  $x^w$  in the above to find the generating function of walks of width  $w$  and with final vertex at height  $h$ . This is, after some simplification,

$$s(k, w) = \sum_{\ell=0}^{\infty} \sum_{s=1}^{\infty} \sum_{i=0}^{\infty} \frac{\ell}{s} \binom{s}{i} \binom{s}{i+\ell} \binom{h}{w-k-s} \binom{w-n+1}{\ell} \frac{y^{h+2i}}{(1-y^2)^s}. \quad (33)$$

Here, the summation over  $s$  is allowed to run to infinity to simplify the expressions. This does not introduce new terms since the binomial coefficients introduce a natural cut-off on the sums. It remains to multiply the above by  $\sigma^k$  and to sum over  $k$  as well – this gives the generating function  $G_{wh}(a, y)$  of walks of width  $w$  ending in a vertex of height  $h$ , and with  $a$  generating steps at height zero.

A minor simplification can be achieved by noting that the sum over  $\ell$  can be done. This reduces the number of summations above to two with the result that

$$s(k, w) = \sum_{s=1}^{\infty} \sum_{i=0}^{\infty} \frac{w+1-s}{n} \binom{n}{i} \binom{h}{w-k-s} \binom{w}{s-i-1} \frac{y^{h+2i}}{(1-y^2)^s}. \quad (34)$$

The  $s=0$  term is equal to  $y^h \binom{h}{w-k}$ , and this should be inserted explicitly in the above. Multiplying this by  $\sigma^k$  and summing over  $k$  gives the generating function for walks of width  $w$  ending a vertex at height  $h$  and with  $a$  generating steps at height zero. After some simplification, this is

$$G_{wh}(a, y) = \sum_{s=0}^w \sum_{k=0}^w \sum_{i=0}^{\infty} \frac{w+1-s}{w+i+1-s} \binom{h}{w-k-s} \binom{n-1}{i} \binom{w}{s-i} \frac{y^{h+2i} (a-1)^k}{(1-y^2)^s}, \quad (35)$$

where the substitution  $\sigma = a-1$  was made.

## 2.2. The partition function

The partition function of adsorbing partially directed walks of width  $w$  can be extracted from  $G_{wh}(a, y)$  in equation (35) by determining the coefficients of  $y^N$  (note that the coefficient of  $y^N$  in  $G_{wh}(a, y)$  is the partition function of walks of length  $w+N$ ). In other words, it remains only to expand  $(1-y^2)^{-s}$  and to collect the coefficient of  $y^N$ . Using the binomial theorem, putting  $n = w+N$ , substituting  $\sigma = a-1$  and simplifying, gives the partition function of partially directed walks with  $w$  horizontal steps and length  $n$ :

$$Z_n(w, h) = \sum_{i=0}^n \sum_{k=0}^w \sum_{s=0}^w \frac{w+1-s}{w+i+1-s} \times \binom{s-1}{i} \binom{w}{s-i} \binom{h}{w-k-s} \binom{-s}{\frac{1}{2}(w+h-n)-s+i} (-1)^{(w+h-n)/2+i} (a-1)^k. \quad (36)$$

This expression can be simplified using standard binomial identities to

$$Z_n(w, h) = \sum_{i=0}^n \sum_{k=0}^w \sum_{s=0}^w \frac{w+1-s}{w+i+1-s} \times \binom{s-1}{i} \binom{w}{s-i} \binom{h}{w-k-s} \binom{\frac{1}{2}(n-w-h)-i+s-1}{s-1} (a-1)^k. \quad (37)$$

For example, if  $n = 8$ ,  $w = 4$  and  $h = 2$ , then

$$Z_8(4, 2) = 30 + 20a + 11a^2 + 4a^3; \quad (38)$$

the partition function of partially directed walks of length 8 and width 4, and with generating variable  $a$  generating edge-visits at height  $h = 0$ . Thus,  $Z_n(w, h)$  is the partition function of *adsorbing partially directed walks* of length  $n$ , width  $w$  and endpoint at height  $h$  (see figure 1).

## 3. The limiting entropic forces

In this section the entropic forces arising in the limit  $n \rightarrow \infty$  are examined. Forces for finite values of  $n$  will be examined in section 4 (for the non-interacting partially directed walk when  $a = 1$ ).

The extrinsic free energy of a walk of length  $n$ , width  $w$ , and endpoint at height  $h$  is given by

$$F_n(w, h) = \log Z_n(w, h) \quad (39)$$

in terms of the partition function in equation (37). This is the free energy of a walk as illustrated in figure 1, confined by two vertical walls a distance  $w$  apart. If the walls are close together (that is, when  $w$  is small), then the walk is constrained, and it loses entropy (this reduces its extrinsic free energy). Similarly, if  $w$  is large, then the walk is stretched in the horizontal direction, and it loses entropy as well. The loss in entropy in both these cases induces a restoring entropic force on the opposing walls in figure 1, moving them further apart (the repulsive regime), or closer together (the attractive regime). At an intermediate distance the entropic force is zero, and this is the *zero force point*.

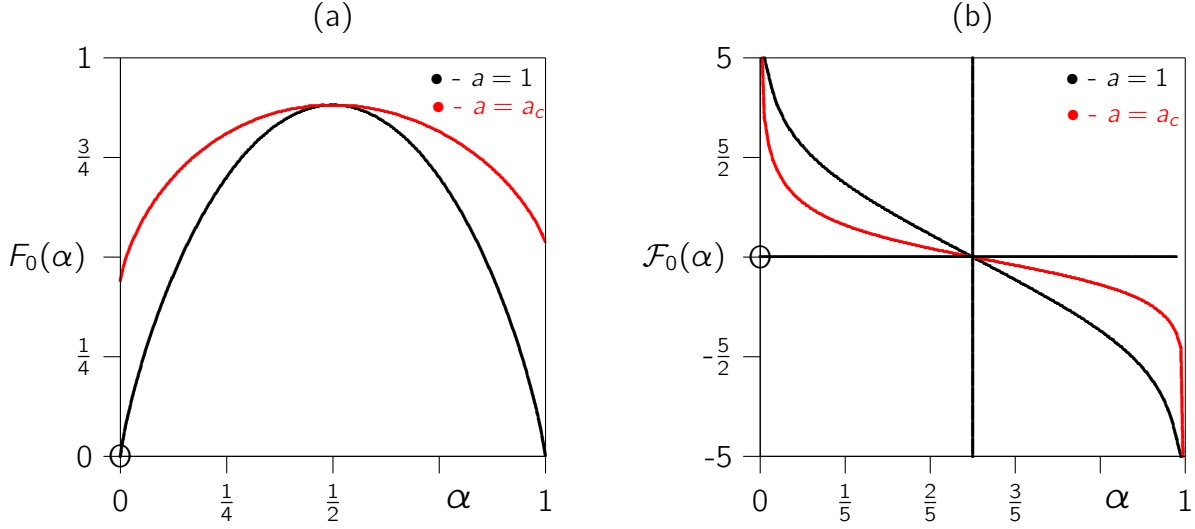


Figure 4: (a) The limiting free energy of a partially directed walk as a function of  $\alpha$ . The bottom curve is the limiting free energy for  $a = 1$  and  $h = 0$ . The top curve is the limiting free energy for  $a = a_c$  and  $h = 0$ . The derivatives of these curves are the limiting entropic force on the vertical walls, and are plotted as a function of  $\alpha$  in (b). The darker curve is the force curve for  $a = 1$  and the lighter curve (lower on the left and higher on the right in (b)) is the force curve for  $a = a_c$ . Both curves pass through the zero force point at  $\alpha = \frac{1}{2}$ . The curve for  $a = 1$  is symmetric on reflection through the point  $(\frac{1}{2}, 0)$ .

### 3.1. Entropic forces on confining walls

The first priority is to determine the limiting (intrinsic) free energy of the walk in the limit  $n \rightarrow \infty$ , after rescaling edges and lengths in the model by  $\frac{1}{n}$  (so that edges have length  $\frac{1}{n}$ , and the vertical walls are a distance  $w = \frac{1}{n} \lfloor \alpha n \rfloor$  apart). In this limit the free energy can be calculated from equation (35), or more appropriately, by considering the exponentially fastest growing terms in equation (37).

For general values of  $a$  and  $h$  it follows from equation (37) that

$$\frac{w+1-s}{w+i+1-s} \binom{s-1}{i} \binom{w}{s-i} \binom{h}{w-k-s} \binom{\frac{1}{2}(n-w-h)-i+s-1}{s-1} (a-1)^k \leq Z_n(w, h),$$

for any  $n > 1$ , for any  $a > 1$ , and for any  $\{i, k, s\}$ . Similarly, if  $\{i_m, k_m, s_m\}$  are the values of  $\{i, k, s\}$  which maximizes the summand on the right hand side of equation (37), then

$$\frac{(n+1)^3(w+1-s_m)}{w+i_m+1-s_m} \binom{s_m-1}{i_m} \binom{w}{s_m-i_m} \binom{h}{w-k_m-s_m} \binom{\frac{1}{2}(n-w-h)-i_m+s_m-1}{s_m-1} (a-1)^{k_m}$$

is an upper bound on  $Z_n(w, h)$ .

Rescale  $(w, h)$  by putting  $w = \lfloor \alpha n \rfloor$ , and  $h = \lfloor \phi n \rfloor$ . The summation indices in the lower bound are similarly scaled by  $s = \lfloor \epsilon n \rfloor$ ,  $i = \lfloor \delta n \rfloor$ , and  $k = \lfloor \kappa n \rfloor$ . Taking the power  $\frac{1}{n}$  and then  $n \rightarrow \infty$ , shows that

$$\sup_{\epsilon, \delta, \kappa} \left[ \frac{\alpha^\alpha \phi^\phi (1-\alpha-\phi-2\delta+2\epsilon)^{(1-\alpha-\phi-2\delta+2\epsilon)/2} (a-1)^\kappa}{2^\epsilon \delta^\delta (\epsilon-\delta)^{2(\epsilon-\delta)} (1-\alpha-\phi-2\delta)^{(1-\alpha-\phi-2\delta)/2} (\phi-\alpha+\kappa+\epsilon)^{\phi-\alpha+\kappa+\epsilon} (\alpha+\delta-\epsilon)^{\alpha+\delta-\epsilon} (\alpha-\kappa-\epsilon)^{\alpha-\kappa-\epsilon}} \right] \quad (40)$$

is a lower bound on  $\lim_{n \rightarrow \infty} Z_n^{1/n}(\lfloor \alpha n \rfloor, \lfloor \phi n \rfloor)$ . In fact, by the above this limit cannot exceed this lower bound for any values of  $(\alpha, \phi) \in [0, 1]^2$ . This supremum is particularly useful in determining the free energy for the cases that  $\phi > 0$  or  $a > a_c$ . Determining

the free energy for  $h = 0$  and  $a = 1$ , or for  $h = 0$  and  $a = a_c = 1 + \frac{1}{\sqrt{2}}$ , requires a similar approach based on equation 37 (but with  $h = 0$ ). These cases are considered in sections 3.1.1 and 3.1.3 below.

*3.1.1. Forces when  $a = 1$  and  $\phi = 0$ :* Putting  $a = 1$  and  $h = 0$  in the summand in equation (37) reduces the partition function to a single sum. The summand is

$$\frac{1}{[\delta n] + 1} \binom{[\alpha n] - 1}{[\delta n]} \binom{[\alpha n]}{[\alpha n] - [\delta n]} \binom{\frac{1}{2}(n + [\alpha n]) - [\delta n] - 1}{[\delta n] - 1}$$

where  $w = [\alpha n]$  and  $i = [\delta n]$ . The limiting free energy is obtained by determining the maximum exponential rate of growth of this summand in the limit that  $n \rightarrow \infty$ . This can be done by using the Stirling approximation for the binomial coefficients, taking the power  $\frac{1}{n}$ , and then taking  $n \rightarrow \infty$ . This gives

$$\frac{\alpha^\alpha (\alpha - 2\delta)^{2\delta} (1 + \alpha - 2\delta)^{(1 + \alpha - 2\delta)/2}}{2^\alpha \delta^{2\delta} (\alpha - \delta)^{2\alpha} (1 - \alpha - 2\delta)^{(1 - \alpha - 2\delta)/2}}. \quad (41)$$

The rate of growth of this is a maximum when  $\delta = \delta_c$  and

$$\delta_c = \frac{1}{2} \pm \frac{1}{2} \sqrt{2\alpha^2 - 2\alpha + 1}. \quad (42)$$

Substituting  $\delta = \delta_c$  gives the limiting free energy as a function of  $\alpha$ :

$$F_0(\alpha) = \alpha \log(2\alpha(1 - \alpha)) - 2\alpha \log(\sqrt{C} + 2\alpha - 1) + \frac{1}{2}\sqrt{C} \log\left(\frac{C + \alpha}{C - \alpha}\right) + (\sqrt{C} - 1) \log\left(\frac{1 - \sqrt{C}}{\sqrt{C} + 2\alpha - 1}\right), \quad (43)$$

where  $C = 2\alpha^2 - 2\alpha + 1$ . Notice that  $F_0(\frac{1}{2}) = \log(1 + \sqrt{2})$ ; this is not unexpected, since partially directed walks grow asymptotically proportionally to  $(1 + \sqrt{2})^{n + o(n)}$ .

The free energy is plotted as a function of  $\alpha$  in figure 4(a). Expanding the free energy about its peak at  $\alpha = \frac{1}{2}$  gives

$$F_0(\alpha) = \log(1 + \sqrt{2}) - 2\sqrt{2}(\alpha - \frac{1}{2})^2 - \frac{2}{3}\sqrt{2}(\alpha - \frac{1}{2})^4 + O((\alpha - \frac{1}{2})^6), \quad (44)$$

where  $O((\alpha - \frac{1}{2})^6)$  is a correction which has leading term  $-\frac{28}{15}\sqrt{2}(\alpha - \frac{1}{2})^6$ .

The derivative of  $\mathcal{F}_0(\alpha) = \frac{d}{d\alpha} F_0(\alpha)$  is the limiting entropic force on the vertical walls confining the walk. Taking the derivative of the approximation in equation (44) to  $\alpha$  gives the force near  $\alpha = \frac{1}{2}$ :

$$\mathcal{F}_0(\alpha) = -4\sqrt{2}(\alpha - \frac{1}{2}) - \frac{2}{3}\sqrt{2}(\alpha - \frac{1}{2})^3 - \frac{7 \cdot 2^3}{5}\sqrt{2}(\alpha - \frac{1}{2})^5 + O((\alpha - \frac{1}{2})^7). \quad (45)$$

More generally, taking the derivative of  $F_0(\alpha)$  in equation (43) gives the limiting force as a function of  $\alpha$ . This is plotted in figure 4(b) and simplifies to

$$\mathcal{F}_0(\alpha) = \log\left(\frac{2\alpha(1 - \alpha)}{(C + 2\alpha - 1)^2}\right) + \frac{C^2 - 2\alpha}{2C} \log\left(\frac{(C - \alpha)(2\alpha + C - 1)^2}{(C + \alpha)(1 - C)^2}\right). \quad (46)$$

It may be verified that  $\mathcal{F}_0(\alpha) = -\mathcal{F}_0(1 - \alpha)$ , so  $\mathcal{F}_0(\frac{1}{2}) = 0$ . That is, the limiting force curve is symmetric on reflection through the point  $(\frac{1}{2}, 0)$ . For small  $\alpha > 0$  the above shows that  $\mathcal{F}_0(\alpha) \sim |\log \alpha|$ ; this will also be shown later (see equation (65)).

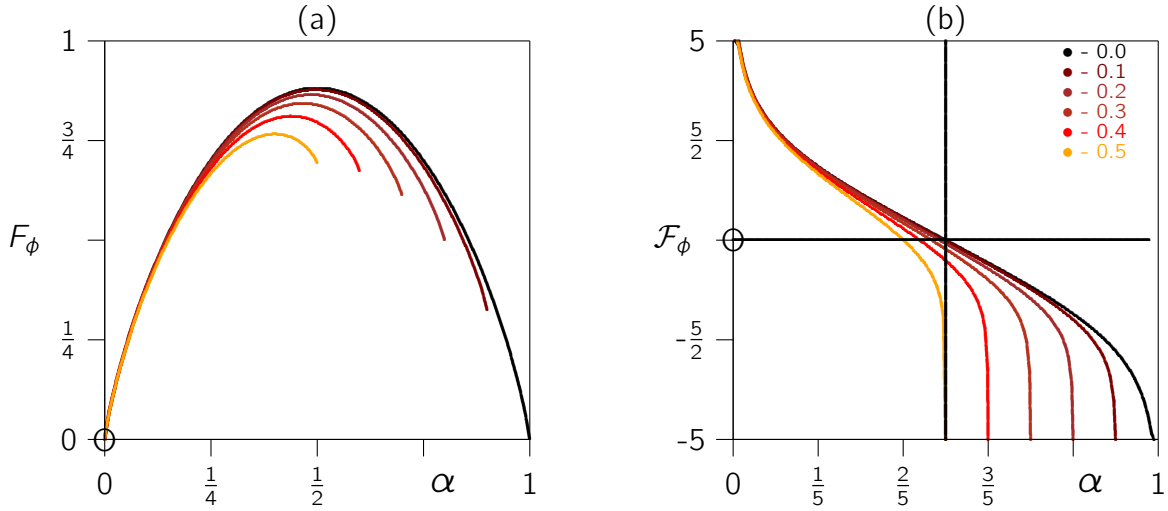


Figure 5: (a) The limiting free energy  $F_\phi(\alpha, \phi)$  plotted as a function of  $\alpha$  for  $\phi \in \{0, 0.1, 0.2, 0.3, 0.4, 0.5\}$ . Notice that  $\alpha \in [0, 1-\phi]$ . (b) Force curves  $\mathcal{F}_\phi(\alpha, \phi)$  as a function of  $\alpha$ . Increasing  $\phi$  moves the zero force point to smaller values of  $\alpha$ . For  $\phi = 0$  the zero force point is located at  $\alpha_c(0) = \frac{1}{2}$ .

3.1.2. *Forces when  $a = 1$  and  $\phi > 0$ :* The limiting free energy can be determined by computing the supremum

$$\sup_{\epsilon, \delta} \left[ \frac{\alpha^\alpha \phi^\phi (1-\alpha-\phi-2\delta+2\epsilon)^{(1-\alpha-\phi-2\delta+2\epsilon)/2}}{2^\epsilon \delta^\delta (\epsilon-\delta)^{2(\epsilon-\delta)} (1-\alpha-\phi-2\delta)^{(1-\alpha-\phi-2\delta)/2} (\phi-\alpha+\epsilon)^{\phi-\alpha+\epsilon} (\alpha+\delta-\epsilon)^{\alpha+\delta-\epsilon} (\alpha-\epsilon)^{\alpha-\epsilon}} \right], \quad (47)$$

which is found after putting  $\kappa = 0$  and by taking  $a \rightarrow 1^-$  in equation (40). The supremum is realised when  $\epsilon = \epsilon_s$ , and  $\delta = \delta_s$ , where  $\epsilon_s$  and  $\delta_s$  are given by (note that  $0 \leq \alpha + \phi \leq 1$ )

$$\epsilon_s = \frac{\alpha(\alpha - \alpha^2 + \sqrt{(2\alpha^2 - 2\alpha + 1)\phi^2 - \phi^4})}{(\alpha + \phi)(1 + \phi - \alpha)} \quad (48)$$

$$\delta_s = \frac{\alpha(1 - \alpha - \phi)(\phi + \phi^2 - \sqrt{(2\alpha^2 - 2\alpha + 1)\phi^2 - \phi^4})}{2\phi(\alpha + \phi)(1 + \phi - \alpha)} \quad (49)$$

Substituting these values to determine the supremum (using Maple [23]) gives a very lengthy expression for the free energy  $F_\phi(\alpha, \phi)$  as a function of  $(\alpha, \phi)$ . It is plotted against  $\alpha$  for various values of  $\phi$  in figure 5(a).

The force  $\mathcal{F}_\phi(\alpha, \phi)$  is the (partial) derivative of  $F_\phi(\alpha, \phi)$  to  $\alpha$ . This is plotted against  $\alpha$  for various values of  $\phi$  in figure 5(b). If  $\phi = 0$  then the force vanishes when  $\alpha = \frac{1}{2}$ , so that  $\mathcal{F}_\phi(\frac{1}{2}, 0) = 0$  (where  $\phi = 0$ ). This is the zero force point for the case  $\phi = 0$ . The zero force point is generally located at  $a_c(\phi)$ , so  $a_c(0) = \frac{1}{2}$ . If  $\phi$  increases, then the zero force point moves to smaller values of  $\alpha$ . By expanding the force in  $\phi$  and  $\alpha$ , the location of the zero force point as a function of  $\phi$  can be estimated by determining the first few terms in a series expansion in  $\phi$ . To order  $\phi^6$  this is

$$\alpha_c(\phi) = \frac{1}{2} - \frac{1}{4}\sqrt{2}\phi^2 + \frac{1}{4}(3\sqrt{2}-2)\phi^4 + \frac{1}{48}(144-149\sqrt{2})\phi^6 + O(\phi^8). \quad (50)$$

This estimate is surprisingly accurate. For example,  $a_c(0.1) = 0.4964\dots$  and the estimate is  $a_c(0.1) \approx 0.4965\dots$ , and  $a_c(0.3) = 0.4669\dots$  while the estimate is  $a_c(0.3) \approx 0.4717\dots$ . The estimate for  $\phi = 0.5$  is  $a_c(0.5) \approx 0.4249\dots$  as opposed to the exact value  $a_c(0.5) = 0.40095\dots$ .

3.1.3. *Forces when  $a = a_c$  and  $\phi = 0$ :* Put  $a = a_c = 1 + \frac{1}{\sqrt{2}}$  in summand in equation (37) and bound the partition function in a way similar to the way it was done in section (3.1). Take the power  $\frac{1}{n}$ , and let  $n \rightarrow \infty$ . This shows that the limiting free energy can be determined by computing critical values of  $(\epsilon, \delta, \kappa)$  to find the supremum

$$\sup_{\epsilon, \delta, \kappa} \left[ \frac{\alpha^\alpha (1-\alpha-2\delta+2\epsilon)^{(1-\alpha-2\delta+2\epsilon)/2} (\frac{1}{\sqrt{2}})^\kappa}{\delta^\delta (\epsilon-\delta)^{2(\epsilon-\delta)} (1-\alpha-2\delta)^{(1-\alpha-2\delta)/2} (\kappa+\epsilon-\alpha)^{\kappa+\epsilon-\alpha} (\alpha+\delta-\epsilon)^{\alpha+\delta-\epsilon} (\alpha-\kappa-\epsilon)^{\alpha-\kappa-\epsilon}} \right]. \quad (51)$$

The critical values of  $(\epsilon, \delta, \kappa)$  in the above are

$$\begin{aligned} \epsilon_s &= \frac{1}{4}(2-\sqrt{2}) \left( 1+\alpha + \sqrt{4\sqrt{2}\alpha(1-\alpha) + (1+\alpha)^2} \right); \\ \delta_s &= \frac{1}{2}(2-\sqrt{2})(1-\alpha); \\ \kappa_s &= \frac{1}{4}(2-\sqrt{2}) \left( (1+\sqrt{2})^2\alpha - 1 - \sqrt{4\sqrt{2}\alpha(1-\alpha) + (1+\alpha)^2} \right). \end{aligned}$$

Substituting these, simplifying, and then taking the logarithm gives a lengthy expression for the limiting free energy  $F_c(\alpha)$  as a function of  $\alpha$ . Expanding this in  $\alpha$  about  $\alpha = \frac{1}{2}$  gives, after simplification,

$$\begin{aligned} F_c(\alpha) &= \log(1+\sqrt{2}) - \frac{4}{7}(2\sqrt{2}-1) \left(\alpha - \frac{1}{2}\right)^2 + \frac{8}{7^3}(\sqrt{2}-1) \left(\alpha - \frac{1}{2}\right)^3 \\ &\quad - \frac{4}{3 \cdot 7^5} (1+\sqrt{2})^2 (1-2\sqrt{2})^6 (1+8\sqrt{2}) \left(\alpha - \frac{1}{2}\right)^4 + O\left(\left(\alpha - \frac{1}{2}\right)^5\right). \end{aligned} \quad (52)$$

Notice that  $F_c(\alpha)$  is not symmetric about  $\alpha = \frac{1}{2}$ , unlike  $F_0(\alpha)$  (the free energy when  $\phi = 0$  and  $a = 1$ ). Taking the derivative of  $F_c(\alpha)$  to  $\alpha$  gives the force near  $\alpha = \frac{1}{2}$ :

$$\begin{aligned} \mathcal{F}_c(\alpha) &= \frac{2^3}{7}(2\sqrt{2}-1) \left(\alpha - \frac{1}{2}\right) + \frac{3 \cdot 2^3}{7^3}(\sqrt{2}-1) \left(\alpha - \frac{1}{2}\right)^2 \\ &\quad - \frac{2^4}{3 \cdot 7^5} (1+\sqrt{2})^2 (1-2\sqrt{2})^6 (1+8\sqrt{2}) \left(\alpha - \frac{1}{2}\right)^3 + O\left(\left(\alpha - \frac{1}{2}\right)^4\right). \end{aligned} \quad (53)$$

The full expression of the free energy  $F_c(\alpha)$  is a lengthy expression determined using Maple [23] and it is plotted in figure 4(a). Taking its derivative to  $\alpha$  shows that the force vanishes when  $\alpha = \frac{1}{2}$ , consistent with the series expansion above. Thus,  $\mathcal{F}_c(\frac{1}{2}) = 0$ . The force curve is plotted in figure 4(b).

3.1.4. *Forces when  $a = a_c$  and  $\phi > 0$ :* If  $a = a_c$  and  $\phi > 0$ , then the critical values of  $(\epsilon, \delta, \kappa)$  in equation (40) are given by

$$\begin{aligned} \epsilon_s &= \frac{1}{4}(2-\sqrt{2}) \left( 1+\alpha-\phi + \sqrt{4\sqrt{2}\alpha(1-\alpha-\phi) + (1+\alpha-\phi)^2} \right); \\ \delta_s &= \frac{1}{2}(2-\sqrt{2})(1-\alpha-\phi); \\ \kappa_s &= \frac{1}{4}(2-\sqrt{2}) \left( (1+\sqrt{2})^2\alpha - 3\phi - 1 - \sqrt{4\sqrt{2}\alpha(1-\alpha-\phi) + (1+\alpha-\phi)^2} \right), \end{aligned}$$

Substituting these into equation (40), simplifying, and then taking the logarithm, gives a lengthy expression for the limiting free energy  $F_c(\alpha, \phi)$  as a function of  $\alpha$  and  $\phi$ . The entropic forces are again given by the partial derivative  $\mathcal{F}_c(\alpha, \phi) = \frac{\partial}{\partial \alpha} F_c(\alpha, \phi)$ .

In figure 6 the limiting free energy and forces are plotted as a function of  $\alpha$  for fixed  $\phi$ . With increasing  $\phi$  the zero force point  $\alpha_c(\phi)$  moves to smaller values of  $\alpha$ . The

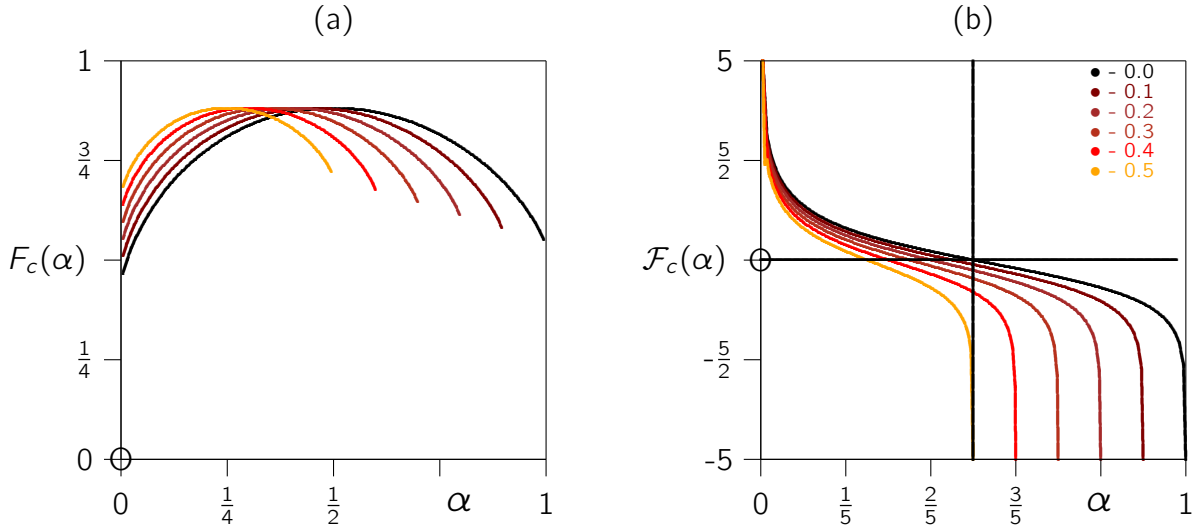


Figure 6: (a) The limiting free energy  $F_c(\alpha)$  plotted as a function of  $\alpha$  for  $\phi \in \{0, 0.1, 0.2, 0.3, 0.4, 0.5\}$ . Notice that  $\alpha \in [0, 1 - \phi]$ . (b) Force curves  $\mathcal{F}_c(\alpha)$  as a function of  $\alpha$ . Increasing  $\phi$  moves the zero force point to smaller values of  $\alpha$ , and this point is located at exactly  $\frac{1}{2} - \frac{1}{2}\phi$ .

location of this point may be approximated by expanding the force in  $\phi$  and in  $\alpha$ , and then solving for  $\alpha$  as a function of  $\phi$ . The result is

$$\alpha_c(\phi) = \frac{1}{2} - \frac{1}{2}\phi + O(\phi^2). \quad (54)$$

Numerical analysis of the model suggests that the correction  $O(\phi^2)$  is zero, so  $\alpha_c(\phi)$  is equal to  $\frac{1}{2} - \frac{1}{2}\phi$ . This is verified by substitution and then simplification of the expression for the force. That is, the zero force point is located exactly at

$$\alpha_c(\phi) = \frac{1}{2} - \frac{1}{2}\phi. \quad (55)$$

if  $a = a_c$ .

**3.1.5. Forces when  $a > a_c$  and  $\phi > 0$ :** The adsorbed phase of the model is obtained if  $a > a_c$ . In this case the critical values of  $(\epsilon, \delta, \kappa)$  in equation (40) are given by

$$\epsilon_s = \frac{1}{4a} \left( 1 + \alpha - \phi + \sqrt{8(a-1)\alpha(1-\alpha-\phi) + (1+\alpha-\phi)^2} \right);$$

$$\delta_s = \frac{1}{2a} (1 - \alpha - \phi);$$

$$\kappa_s = \frac{1}{4a} \left( (4a-1)\alpha - 3\phi - 1 - \sqrt{8(a-1)\alpha(1-\alpha-\phi) + (1+\alpha-\phi)^2} \right),$$

provided that  $a > a_c$ .

Notice that  $\epsilon_s + \kappa_s = \alpha - \frac{1}{a}\phi \leq \alpha$  as required in equation (40), provided that  $a\alpha \geq \phi$ . Similarly,  $\phi - \alpha + \epsilon_s + \kappa_s = \phi(1 - \frac{1}{a}) \geq 0$ , provided that  $a \geq 1$ . In addition,  $\epsilon_s \geq \delta_s$  and  $1 - \alpha - \phi - 2\delta_s \geq 0$  if both  $a \geq 1$  and  $\alpha + \phi \leq 1$ .

Substitution of the above critical values for  $(\epsilon, \delta, \kappa)$  and taking the logarithm gives the limiting (intensive) free energy  $F(\alpha, \phi)$ . This expression for  $F(\alpha, \phi)$  is lengthy (it was determined using Maple [23]) and will not be reproduced here.

Taking the derivative of  $F(\alpha, \phi)$  to  $\alpha$  gives the limiting entropic force  $\mathcal{F}(\alpha, \phi)$ . Putting both  $\phi = 0$  and  $a = 1$  simplifies  $\mathcal{F}(\alpha, \phi)$  to equation (46), and this force is plotted in figure 7(a).

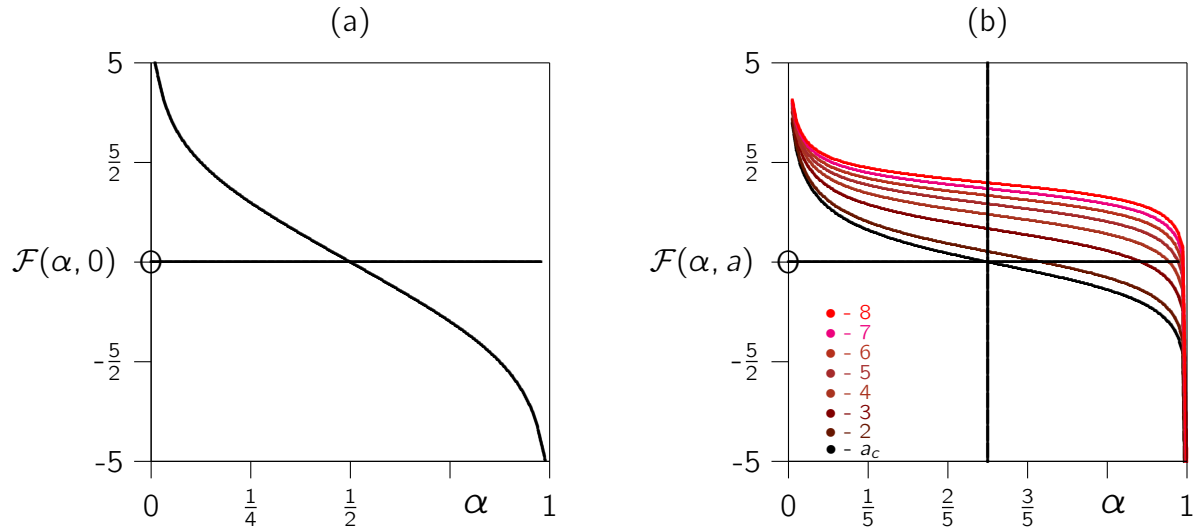


Figure 7: (a) The entropic force curve for  $a = 1$  and  $\phi = 0$  is recovered from the force  $\mathcal{F}(\alpha, 0)$ . This curve is identical to the force curve  $\mathcal{F}_0$  for  $a = 1$ , plotted in figure 4(b). (b) The force curves  $\mathcal{F}(\alpha, a)$  for increasing values of  $a$ . If  $a = a_c$ , then the zero force point is at  $\alpha = \frac{1}{2}$ . Increasing  $a$  moves the zero force point to the right and flattens the force curve, compared to the force curve  $\mathcal{F}_0$  plotted in (a).

In figure 7(b) the forces for values of  $\phi = 0$  and  $a \geq a_c$  and for  $\phi = 0$  are plotted. The expressions for these forces are lengthy, and were obtained using Maple [23]. At the critical adsorption point  $a_c = 1 + \frac{1}{\sqrt{2}}$  the zero force point is located at  $\alpha = \frac{1}{2}$ , unchanged from its location when  $a = 1$ .

Increasing the value of  $a$  gives force curves which are progressively higher in the graph (and so larger if repulsive, and less attractive, if attractive), while the zero force point moves towards larger values of  $\alpha$ . If  $\phi = 0$ , then the location of the zero force point may be estimated by expanding the force in  $\alpha$  and solving for the zero force point. This gives the following asymptotic expression for the location of the zero-force point: If  $a - a_c$  is small, then the zero force point is located at

$$\alpha_c(a) = \frac{1}{2} + \frac{1}{2}(a - a_c) - \frac{1}{4}(\sqrt{2} - 1)(a - a_c)^2 + O((a - a_c)^3). \quad (56)$$

For example, if  $a = a_c + 0.1$ , then  $\alpha_c(a_c + 0.1) = 0.5488 \dots$  while the approximation gives  $\alpha_c(a_c + 0.1) \approx 0.544 \dots$ . Similarly,  $\alpha_c(a_c + 0.05) = 0.5247 \dots$  while the approximation gives  $\alpha_c(a_c + 0.05) \approx 0.524 \dots$ .

For large values of  $a$  an asymptotic expression for the zero force point may be found. This is given by

$$\alpha_c(a) = 1 - \frac{2}{(a-1)^3} + \frac{4}{(a-1)^4} - \frac{10}{(a-1)^5} + O((a-1)^{-6}). \quad (57)$$

This becomes very accurate for large values of  $a$ . Numerically  $\alpha_c(4.0) = 0.9559 \dots$  while the above approximation gives  $\alpha_c(4.0) \approx 0.934 \dots$ . Similarly,  $\alpha_c(6.0) = 0.9884 \dots$  while the approximation gives  $\alpha_c(6.0) \approx 0.987 \dots$ .

#### 4. Finite size asymptotics for $a = 1$ and $h = 0$

In this section an asymptotic expression for the partition function in equation (37) (this is for the special case that  $a = 1$  and  $h = 0$ ) is determined. Notice that if  $h = 0$  then



only terms with  $w - k - s = 0$  survive, and if  $a = 1$ , then  $k = 0$ , so that  $w = s$ . This reduces the triple summation in equation (37) to a single summation:

$$Z_n(w, 0) = \sum_{i=0}^w \frac{1}{i+1} \binom{w-1}{i} \binom{w}{w-i} \binom{\frac{1}{2}(n+w)-i-1}{w-1} \quad (58)$$

This partition function will be approximated by an integral, and the integral will be approximated by a saddle point formula. The first step is to find a good approximation for the summand.

Thus, consider the summand in equation (58) and denote it by  $S$ . Its binomial coefficients will be approximated by using the Stirling approximation for the factorial:

$$n! = \sqrt{2\pi n} n^n e^{-n} \left(1 - \frac{1}{12n} + \frac{1}{288n^2} + O\left(\frac{1}{n^3}\right)\right). \quad (59)$$

Take the logarithm of the summand in equation (44) and expand the binomial coefficients into factorials. This gives

$$\begin{aligned} \log S &= \log(i+1) - \log(w-i) + \log\left(\left(\frac{1}{2}(n+w)-i-1\right)!\right) \\ &\quad - \log\left(\left(\frac{1}{2}(n+w)-i-1\right)!\right) - 2\log\left((w-i-1)!\right) + \log(w!) - 2\log((i+1)!). \end{aligned} \quad (60)$$

Substitute the factorial by the Stirling approximation above, and simplify. This gives an expression approximating the logarithm of the summand.

In order to implement a saddle point approximation, it is necessary to find the location of the saddlepoint in the summand. Thus, in the simplified approximation of  $\log S$  above, substitute  $n = \frac{1}{\epsilon}$ ,  $i = \frac{\delta}{\epsilon}$  and  $w = \frac{\alpha}{\epsilon}$ . Expand the resulting expression in  $\epsilon$  and collect the leading term (which is  $O(\epsilon^{-1})$ ). This is a lengthy expression in  $\delta$  and  $\alpha$ , and the saddle point is located by taking its derivative with respect to  $\delta$  and solving for the stationary point. This gives  $\delta = \frac{1}{2} \pm \frac{1}{2} \sqrt{2\alpha^2 - 2\alpha + 1}$  as the possible locations of the saddle point(s) (see for example equation (42)). Notice that the choice of the plus sign before the square root gives  $\delta > \alpha$  – so that  $i > w$  in the summand. This is outside the range of  $i$  in equation (44), with the result that the minus sign before the square root is the correct choice of the sign. Thus, the saddle point is located at asymptotic values of  $i$  in the summand where  $i = \lfloor \delta_s n \rfloor$ , where

$$\delta_s = \frac{1}{2} - \frac{1}{2} \sqrt{2\alpha^2 - 2\alpha + 1}. \quad (61)$$

Numerical work shows that the width in the peak about  $\delta_s$  is proportional to  $\sqrt{n}$ , thus the summation in equation (44) will be approximated by an integral by putting  $n = \frac{1}{\epsilon^2}$ ,  $w = \frac{\alpha}{\epsilon^2}$  and  $i = \frac{\delta_s}{\epsilon^2} + \frac{\delta}{\epsilon}$  in the logarithm of the summand. The result is expanded in a Laurent series in  $\epsilon$ ; this gives leading terms of order  $O(\frac{1}{\epsilon^2})$  and  $O(\frac{1}{\epsilon})$ . The series is truncated to  $O(\epsilon)$ , then exponentiated and simplified, before it is integrated over  $\delta$ . The result will be a saddle point approximation to the partition function  $Z_n(w, 0)$  with  $w = \lfloor \alpha n \rfloor$ , once the substitution  $\epsilon = \frac{1}{\sqrt{n}}$  is made. After significant symbolic computations calculations using Maple [23], the approximation to  $Z_n(w, 0)$  for  $a = 1$  is

$$\begin{aligned} Z_n(\lfloor \alpha n \rfloor, 0) &\sim \frac{1 - \alpha + \alpha^2 + \sqrt{C}}{\pi n^2 \alpha (\alpha - 1)^2 \sqrt{(1 - \alpha)\sqrt{C} + C}} \\ &\quad \times \left( \frac{1 - 3\alpha + 3\alpha^2 + (1 - 2\alpha)\sqrt{C}}{\alpha^\alpha (1 - \alpha)^\alpha} \right)^n \left( \frac{\sqrt{C} + \alpha}{\sqrt{C} - \alpha} \right)^{n/2}, \end{aligned} \quad (62)$$

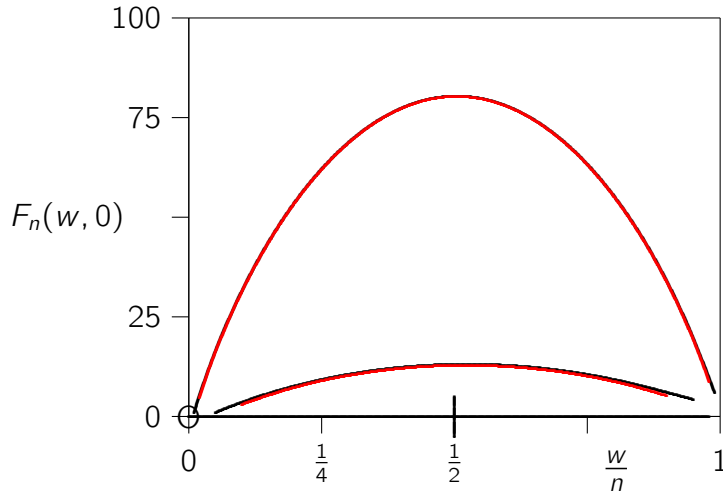


Figure 8: The exact and approximate free energies  $F_n(w, 0)$  for  $n = 20$  (bottom curves) and  $n = 100$  (top curves). The approximate expression is obtained by  $F_n(w, 0) = \log Z_n(w, 0)$  where  $Z_n(w, 0)$  is approximated by equation (62). On this scale there is little differences between the exact curve and its approximation.

where  $C = 2\alpha^2 - 2\alpha + 1$ .

The approximation for  $Z_n$  above also approximates the extensive free energy, given by  $F_n(\lfloor \alpha n \rfloor, 0) = \log Z_n(\lfloor \alpha n \rfloor, 0)$  according to equation (39). In figure 8 the exact extensive free energy, and its approximation (by the logarithm of the right hand side of equation (62)), are plotted on the same graph as a function of  $\frac{w}{n}$  for  $n = 20$  and  $n = 100$ . On the scale of this plot, the approximation is indistinguishable from the exact curve.

An asymptotic formula for the entropic force is obtained by taking the derivative of  $\log Z_n(\lfloor \alpha \rfloor, 0)$  in equation (62) to  $\alpha$  while recalling that  $w = \lfloor \alpha n \rfloor$ . In figure 9 the exact force curve, and the asymptotic approximation to it, are plotted on the same graph for  $n = 200$ . This shows that the forces are very small for  $\alpha = \frac{1}{2}$ . In fact, taking the logarithm and then the derivative of the right hand side of equation (62), gives a complicated expression which simplifies to  $1 + \sqrt{2}$  if  $\alpha = \frac{1}{2}$ . That is, there is no dependence on  $n$  at this point, and it may be verified, using symbolic computations [23], that the coefficient of  $n$  vanishes at this point. That is, the asymptotic expression of the finite size force is of the form

$$\mathcal{F}_n(\alpha) \sim A_\alpha + B_\alpha n \quad (63)$$

and  $A_\alpha$  and  $B_\alpha$  are functions of  $\alpha$  such that  $A_{1/2} = 1 + \sqrt{2}$  and  $B_{1/2} = 0$ . Thus the force does not vanish at  $\alpha = \frac{1}{2}$ , but is, instead, a constant value, independent of  $n$ , where  $\mathcal{F}_n(\frac{1}{2}) = 1 + \sqrt{2}$ . Since  $\mathcal{F}_n(\alpha)$  increases with  $n$  for  $\alpha \neq \frac{1}{2}$ , this indicates that

$$\frac{\mathcal{F}_n(\frac{1}{2})}{\mathcal{F}_n(\alpha)} \rightarrow 0, \text{ as } n \rightarrow \infty \text{ and } \alpha \neq \frac{1}{2}. \quad (64)$$

One may similarly use equation (62) to determine an asymptotic expression for the entropic force on the two vertical walls in figure 1. This may be done by taking the derivative of the free energy to  $\alpha$ . For  $\alpha$  small the result is

$$\mathcal{F}_n(\alpha) \sim -\frac{1}{\alpha} + (n - \frac{1}{2}) - n \log \alpha + O(n\alpha). \quad (65)$$

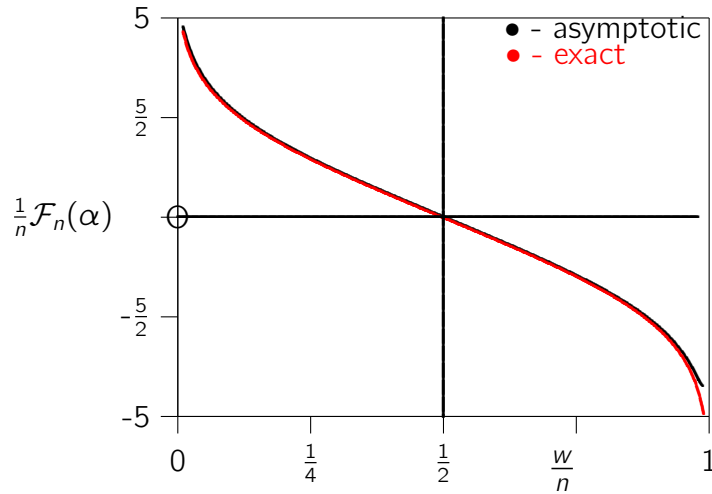


Figure 9: The normalised force curve  $\frac{1}{n}\mathcal{F}_n(\alpha)$  for  $n = 200$  and  $a = 1$  (see figure 2(b)) plotted as a function of  $w$ . There are two curves, namely, the exact force for  $n = 200$ , computed from equation (66), and the asymptotic approximation to  $\mathcal{F}_n(\alpha)$  for  $n = 200$ . The curves pass very close to  $\frac{1}{2}$  when  $\mathcal{F}_n = 0$ .

Fixing  $w = \lfloor n\alpha \rfloor$  and then taking  $\alpha \rightarrow 0^+$  shows that  $\mathcal{F}_n(\alpha) \sim n |\log \alpha| \rightarrow \infty$  for small values of  $n$ . Moreover,  $\frac{1}{n}\mathcal{F}_n(\alpha) \sim |\log \alpha|$  (see section 3.1.1).

## 5. Numerical calculation of the entropic forces

### 5.1. Entropic force on the vertical wall

For finite values of  $n$  and  $w$  the entropic force may be defined by the finite difference

$$\mathcal{F}_n(w, h) = \frac{1}{2} (F_n(w+2, h) - F_n(w, h)) \quad (66)$$

of the extensive free energy. The difference between the free energies for widths  $w+2$  and  $w$  are used in order to avoid parity effects in the model; these parity effects are due to fact that the underlying square lattice is a bipartite graph.

**5.1.1. The case  $a = 1$ :** In this case there is no attraction between the walk and the adsorbing line, and the model is in its desorbed phase.

In figure 2(a) the entropic force  $\mathcal{F}_{20}(w, 0)$  is interpolated on discrete points as a function of the width  $w$  for walks of length  $n = 20$  and endpoint fixed at height  $h = 0$ . As expected, the force between the confining walls is large positive (repulsive) for small values of  $w$ , and large negative (attractive) for large values of  $w$ . At a critical value of  $w$ , namely  $w \approx 10$ , the force is zero, neither attractive nor repulsive.

Forces of paths of different lengths  $n$  can be compared by scaling  $w$  by  $n$  in figure 2(a). In figure 2(b) the interpolated force curves for  $n \in \{20, 40, 60, 80, 100\}$  are plotted against  $\alpha = \frac{w}{n}$ . These curves collapse to a single curve, namely a universal force curve which is the limiting force in the limit  $n \rightarrow \infty$  with length rescaled by  $n$ .

Note that the force curves in figure 2 pass very close to the point  $(w, n) = (\frac{1}{2}n, n)$  when  $\mathcal{F}_n(w, 0) = 0$ . That is, the force is approximately zero when  $w = \frac{1}{2}n$ , or when the confining walls are  $w = \frac{1}{2}n$  apart. This occurs when the walk gives  $\frac{1}{2}n$  horizontal steps,

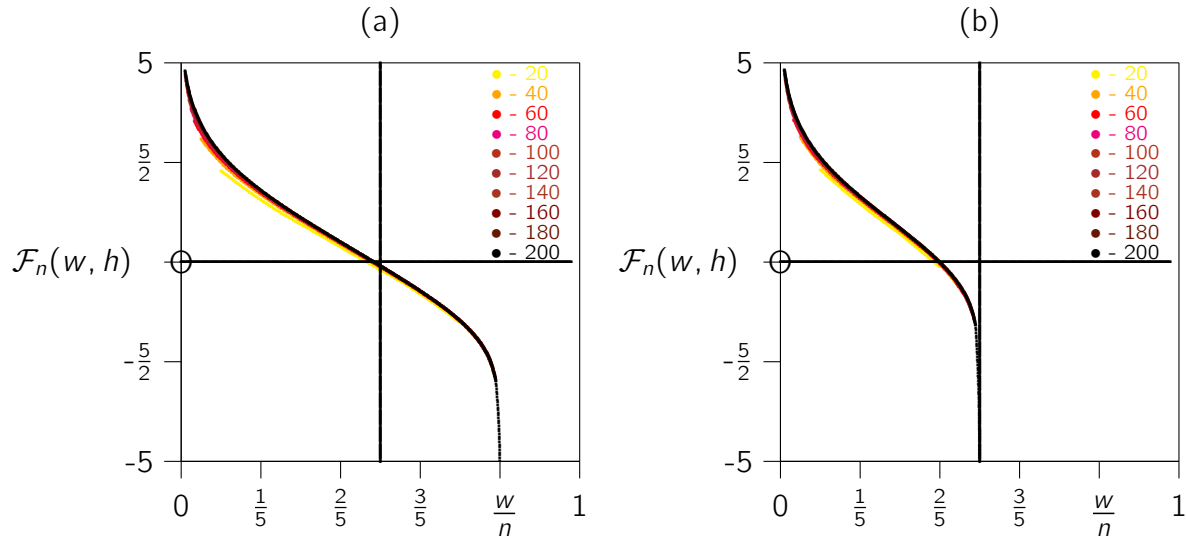


Figure 10: The entropic forces exerted by a partially directed walk between two vertical walls. The width  $w$  of the walk (or distance between the confining walls) is rescaled by  $n$  (the length of the walk). (a) The entropic forces for  $n$  between 20 and 200 plotted for walks with  $a = 1$  and height of endpoint  $h = \frac{1}{5}n$ . Notice that this distorts the curves when  $\frac{w}{n}$  is larger than about 0.5. (b) Similar to (a), but now with  $h = \frac{1}{2}n$ .

and this is consistent with the location of the zero force point at  $\alpha = \frac{1}{2}$  determined in section 3.1.1.

The convergence of the finite size forces to the limiting force curve is quick, this can be seen, for example, in figure 9, where the limiting force, and the exact force for  $n = 200$ , are plotted on the same graph. These curves are indistinguishable on this scale.

In figure 10 the effects of the height of the endpoint on the induced forces are displayed. In figure 10(a) the force curves are plotted for  $h = \lfloor \phi n \rfloor$  with  $\phi = \frac{1}{5}$ . Since  $w$  is rescaled by  $n$ , the curves again collapse to an underlying force curve. For small values of  $w$  the force curves are not changed significantly from those in figure 2(b). In figure 10(b) similar data are presented, but now with  $h = \frac{1}{2}n$ .

Finally, the effects of the adsorption activity  $a$  is examined in figures 11(a) and 11(b). For  $a$  larger than 1 the walks are attracted to the adsorbing boundary  $\partial\mathbb{L}_+^2$ , and they adsorb at  $a = a_c = 1 + \frac{1}{\sqrt{2}}$ . In figure 11(a) the forces are plotted for  $a = 2 > a_c$ . The data shows a longer range of repulsive forces, and for large  $w$ , when the forces are attractive, the magnitude of the forces are reduced. This distortion of the forces can be seen even in the case that  $a = a_c$ , as shown in figure 11(b), although here it is more subtle. There are, however, an apparent reduction in the magnitude of the attractive forces when  $w$  approaches  $n$ .

## 5.2. The pressure on the adsorbing wall

Let  $u = \langle (w, 0) \sim (w+1, 0) \rangle$  be an edge in the adsorbing boundary  $\partial\mathbb{L}_+^2$  a distance  $w$  from the origin. The pressure  $\Pi_n(w)$  on  $u$  is the change in extensive free energy if  $u$  is a blocked so that walks cannot pass through it. That is, if  $f_n$  is the free energy of walks of length  $n$ , and  $f_n(u)$  is the free energy of walks avoiding the edge  $u$ , then the pressure

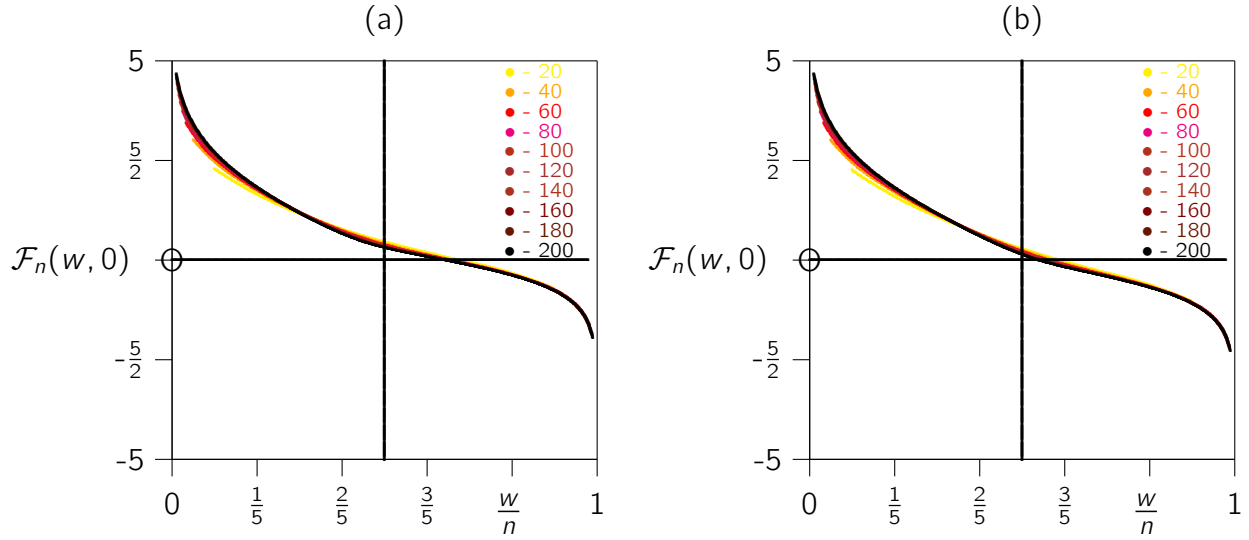


Figure 11: The entropic forces exerted by a partially directed walk between two vertical walls. The width  $w$  of the walk (or distance between the confining walls) is rescaled by  $n$  (the length of the walk) and the height of the endpoint of the walk is at  $h = 0$ . (a) The entropic forces plotted for  $a = 2$ . The force curves are shifted in the positive direction compared to the results in figure 2(b). This shows that the forces are repulsive for larger values of  $w$ , and, when they become attractive (negative), then they are weakened. (b) The entropic forces plotted for  $a = a_c$  (the critical adsorption point in the model).

on  $u$  is given by

$$\Pi_n(w) = f_n - f_n(u). \quad (67)$$

The (extensive) free energies  $f_n$  and  $f_n(u)$  are determined by the corresponding partition functions, and the partition function of walks avoiding  $u$  will be found by first computing the partition function of walks passing through  $u$ .

As in equation (37), denote the partition function of partially directed walks of length  $n$  from the origin in  $\mathbb{L}_+^2$ , with edge-visits to  $\partial\mathbb{L}_+^2$  weighted by  $a$ , of horizontal width  $w$  and with endpoint at height  $h$ , by  $Z_n(w, h)$ . This partition function can be used to determine the partition function of walks passing through an edge  $u$  as illustrated in figure 12.

Let  $b_n(v, h)$  be the number of partially directed walks of length  $n$  in  $\mathbb{L}_+^2$ , from the origin, making  $v$  edge-visits to  $\partial\mathbb{L}_+^2$ , and with final vertex at vertical height  $h$ . The partition function of this walk is given by

$$B_n(h) = \sum_{v=0}^n b_n(v, h) a^v, \quad (68)$$

and it is implicitly a function of the adsorbing activity  $a$ . If  $\mu$  is introduced as the generating variable conjugate to  $h$ , and  $t$  is conjugate to  $n$ , then the generating function of this walk is given by

$$B(t, \mu, a) = \frac{t(1-\mu t) (1 - (1+2\mu)t + t^2 + t^3 - \sqrt{D})}{((1+\mu+\mu^2)t - (1+t^2+t^3)\mu) ((1+a)t^2 + (1-a)(1-t+t^3-\sqrt{D}))} \quad (69)$$

Summing  $B_n(h)$  over  $h$  gives the partition function of walks ending at any height, namely  $P_n = \sum_{h=0}^n B_n(h)$ , and this is also implicitly a function of  $a$ .

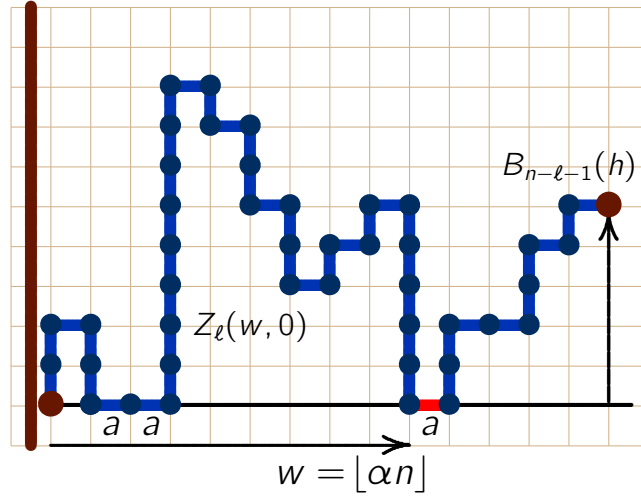


Figure 12: A partially directed walk passing through an edge in the adsorbing boundary a distance  $w$  from the origin may be calculated by concatenating a bargraph path of width  $w$  with a partially directed walk as shown. The bargraph path and partially directed walk are joined by inserting an edge-visit  $u = \langle (w, 0) \sim (w+1, 0) \rangle$  between the endpoint of the bargraph path and the first vertex in the partially directed walk. Since  $u$  is an edge-visit, it carries weight  $a$ , similar to other edge-visits in the model.

Notice that in terms of  $Z_n(w, h)$ ,

$$B_n(h) = \sum_{w=0}^n Z_n(w, h), \text{ and } P_n = \sum_{w=0}^n \sum_{h=0}^{n-w} Z_n(w, h). \quad (70)$$

The partition function of adsorbing bargraph paths is  $B_n(0)$ .

The partition function of walks passing through the edge  $u$  may be obtained concatenating a bargraph path of width  $w$ , with a partially directed walk ending in a vertex at height  $h$ . That is, concatenate a walk generated by  $Z_\ell(w, 0)$  with a path generated by  $B_{n-\ell-1}(h)$ , as illustrated in figure 12, and then sum over  $\ell$ . That is, the partition function of walks passing through the edge  $u$  and ending in a vertex at height  $h$  is

$$Y_n^{(1)}(h) = a \sum_{\ell=w}^{n-1} Z_\ell(w, 0) B_{n-\ell-1}(h). \quad (71)$$

Similarly, for walks ending in a vertex at any height, the partition function is given by

$$Y_n^{(2)} = a \sum_{\ell=w}^{n-1} Z_\ell(w, 0) P_{n-\ell-1}. \quad (72)$$

Note that the extra factor  $a$  in these expressions is the weight of the edge  $u$ , which is not accounted for in the partition function otherwise. See figure 12 for more explanation.

The pressure on the edge  $u$  by walks of length  $n$  can be found from equation (67) by determining  $f_n$  and  $f_n(u)$ . In particular, for walks ending a vertex at height  $h$ ,  $f_n \equiv \log B_n(h)$ , and  $f_n(u) \equiv \log(B_n(h) - Y_n^{(1)}(h))$  since the partition function of walks ending in a vertex at height  $h$  which avoids the edge  $u$  is  $B_n(h) - Y_n^{(1)}(h)$ . Thus the pressure on  $u$  by walks ending in a vertex at height  $h$  is given by

$$\Pi_n^{(1)}(w, h) = \log B_n(h) - \log (B_n(h) - Y_n^{(1)}(h)) = -\log \left( 1 - \frac{Y_n^{(1)}(h)}{B_n(h)} \right). \quad (73)$$

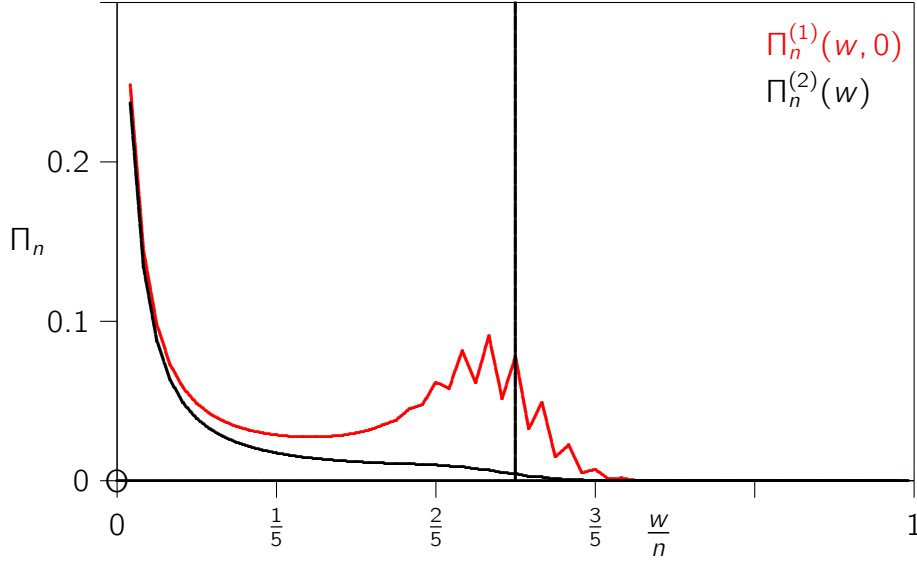


Figure 13: The pressures  $\Pi^{(1)}(w, 0)$  and  $\Pi^{(2)}(w)$  as a function of  $w$ . Notice that  $w$  is normalised by  $n$  and that the pressures are scaled by multiplication with  $n$ . In these simulations  $a = 1$  and  $n = 100$ . The pressure of a bargraph path  $\Pi^{(1)}(w, 0)$  on an edge  $u$  in the adsorbing line at first decreases quickly with increasing  $w$ , but then goes through a secondary, peak strongly modified by a parity effect, at about  $w = \frac{1}{2}n$ . For  $w$  approaching  $n$  the pressure decreases to zero. The pressure of partially directed walks  $\Pi^{(2)}(w)$  with unrestricted endpoint decreases monotonically with increasing  $w$  to small values for  $w > \frac{1}{2}n$ .

Next, the pressure  $\Pi_n^{(1)}(w, 0)$  in equation (73) can be approximated by approximations of  $Y_n^{(1)}(0)$  (see equation (71)) and the bargraph partition function  $B_n(0)$ .  $Y_n^{(1)}(0)$  is approximated by using the asymptotic approximation (62) for  $Z_n(w, 0)$ , and for  $B_n(0)$  the asymptotic approximation

$$B_n(0) \sim \frac{1}{\sqrt{\pi n^3}} \left(1 + \sqrt{2}\right)^{n+3/2} \left(1 - \frac{36+21\sqrt{2}}{16n} + \frac{1745+1260\sqrt{2}}{256n^2} + O(n^{-3})\right), \quad (74)$$

derived in reference [18], can be used. Substitute these in equation (71), and approximate the summation by an integral (notice that the summation in equation (71) includes values of  $\ell$  close to zero, and again close to  $n$ , where the approximations in equations (62) and (74) are poor). Thus, by restricting the summation to  $w > 4$ , the resulting approximation will be

$$Y_n^{(1)}(0) \simeq a \sum_{\ell=w+1}^{n-5} Z_\ell(w, 0) B_{n-\ell-1}(0). \quad (75)$$

That is, using this approximation, and the approximation for  $B_n(0)$  above,  $\Pi_n^{(1)}(w, 0)$  may be approximated using equation (73). This approximation is interpolated on odd values of  $w$  for  $n = 100$  in figure 14 (there are strong parity effects, as seen in figure 13).

Similarly, the pressure of walk ending in a vertex at any height on the edge  $u$  is given by

$$\Pi_n^{(2)}(w) = \log P_n - \log (P_n - Y_n^{(2)}) = -\log \left(1 - \frac{Y_n^{(2)}}{P_n}\right), \quad (76)$$

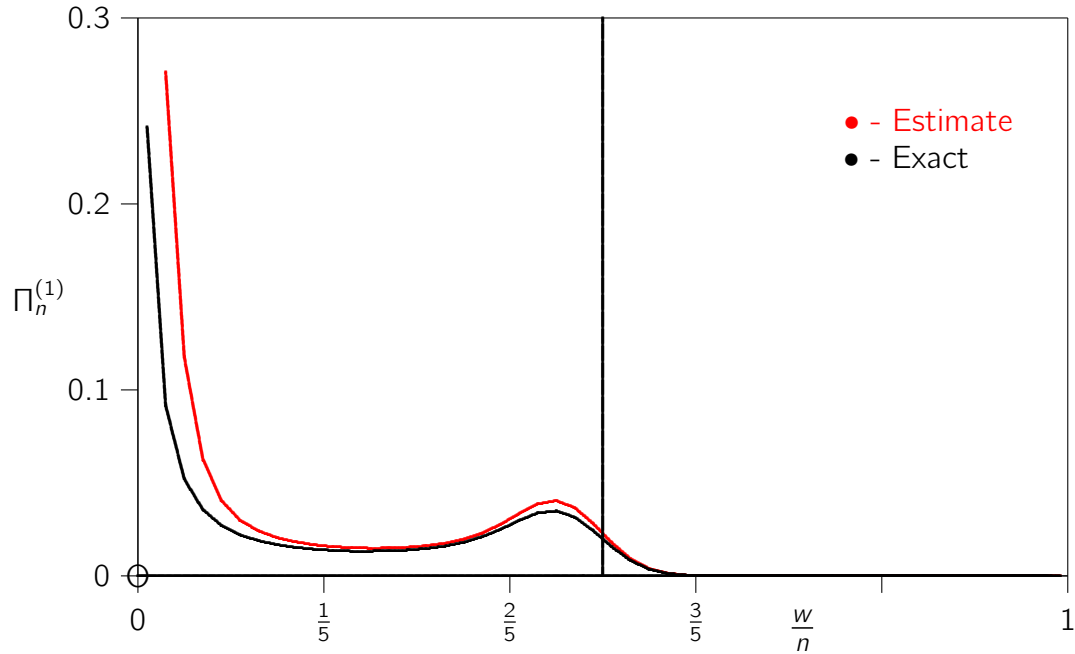


Figure 14: The pressure  $\Pi_n^{(1)}(w, 0)$  of bargraph paths of length  $n = 100$  and  $a = 1$  on  $\partial\mathbb{L}_+^2$  interpolated on odd values of  $w$ . The pressure is large close to the origin, declines steeply with increasing  $w$ , and then passes through a secondary peak before decaying to zero. The estimated pressure were computed by using the approximation in equations (74) and (75) in equation (73).

since  $f_n \equiv P_n$  in equation (67) (where  $P_n$  is the partition function of partially directed walks of length  $n$  ending at any height), and  $f_n(u) \equiv P_n - Y_n^{(2)}$  is the partition function of walks of length  $n$  ending at any height, and avoiding the edge  $u$ .

The pressures  $\Pi_n^{(1)}(w, h)$  and  $\Pi_n^{(2)}(w)$  can be computed for small values of  $n$  (say  $n \leq 100$ ) and involves quadruple summations (three in equation (37) and another in equation (70)). These expressions were coded into a C program in order to explore the pressures  $\Pi^{(1)}$  and  $\Pi^{(2)}$ . Numerical simulations for  $a = 1$  show a strong parity dependence on  $w$  (the distance of the edge  $u$  from the origin). For example, in figure 13 the pressures are displayed as a function of  $w$  (normalised by  $n$ ) for  $n = 100$ . The pressure  $\Pi_n^{(1)}(w, 0)$  decreases quickly with increasing  $w$ , but shows a secondary peak for  $w$  approaching  $\frac{1}{2}n$ , with a strong correction due to parity effects. The pressure  $\Pi_n^{(2)}(w)$ , for walks with endpoint at any height, decreases monotonically to zero with increasing  $w$ . Parity effects for small values of  $n$  remains visible in the results; thus, in order to suppress these, pressures were evaluated only for odd values of  $w$ , in what follows below.

In figure 15(a) the pressure  $\Pi_n^{(1)}(w, 0)$  for bargraph walks are interpolated on odd values of  $w$  and plotted against  $\frac{w}{n}$  for  $n \in \{20, 40, 60, 80, 100\}$ . For any fixed  $n$  the pressure decreases with increasing  $w$ , but there is a secondary peak in the pressure when  $w$  approaches  $\frac{1}{2}n$ . The appearance of this secondary peak may be understood by noting that the endpoint of bargraph paths in  $\partial\mathbb{L}_+^2$  would cluster around the expected horizontal width of the path, and so exerts pressure on edges in this vicinity.

It is also noticeable that for fixed values of  $\frac{w}{n}$  the pressure declines with increasing  $n$ . This follows because, with increasing  $n$ , the likelihood of a walk passing through the edge  $u = \langle w \sim (w+1) \rangle$  decreases. Since the rescaling of  $w$  by  $n$  effectively gives



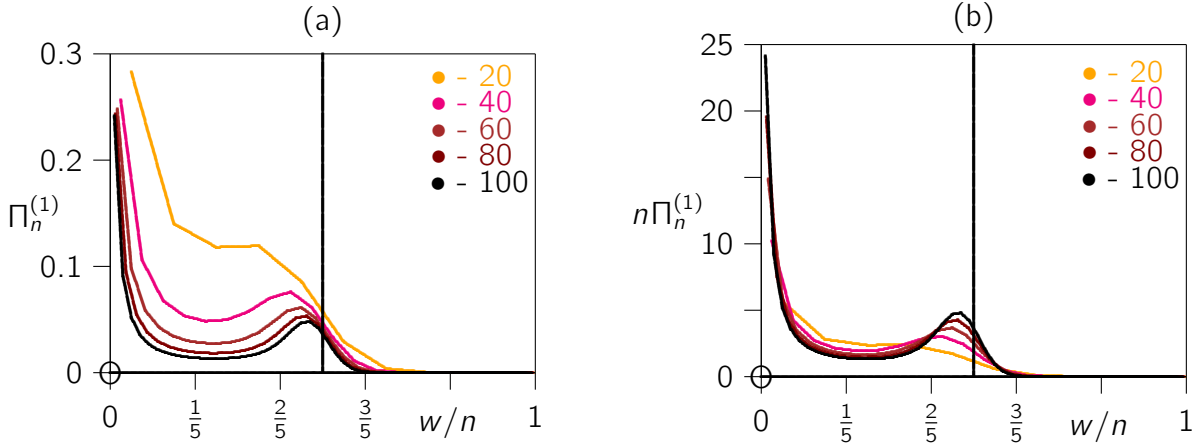


Figure 15: The pressures  $\Pi_n^{(1)}(w, 0)$  as a function of  $w$  with  $a = 1$ . (a) The pressures for  $n$  in  $\{20, 40, 60, 80, 100\}$  against  $\frac{w}{n}$ . With increasing  $n$  the pressure decreases, but it shows a secondary peak when  $w$  approaches  $\frac{1}{2}n$ . (b) Since the length of a rescaled edge decreases proportional to  $\frac{1}{n}$  with increasing  $n$ , the pressures in (a) can be rescaled by plotting  $n\Pi_n^{(1)}$  against  $\frac{w}{n}$ . This brings the data in (a) closer together and suggests an underlying limiting rescaled pressure. Note that the data in these graphs are interpolated on odd values of  $w$ .

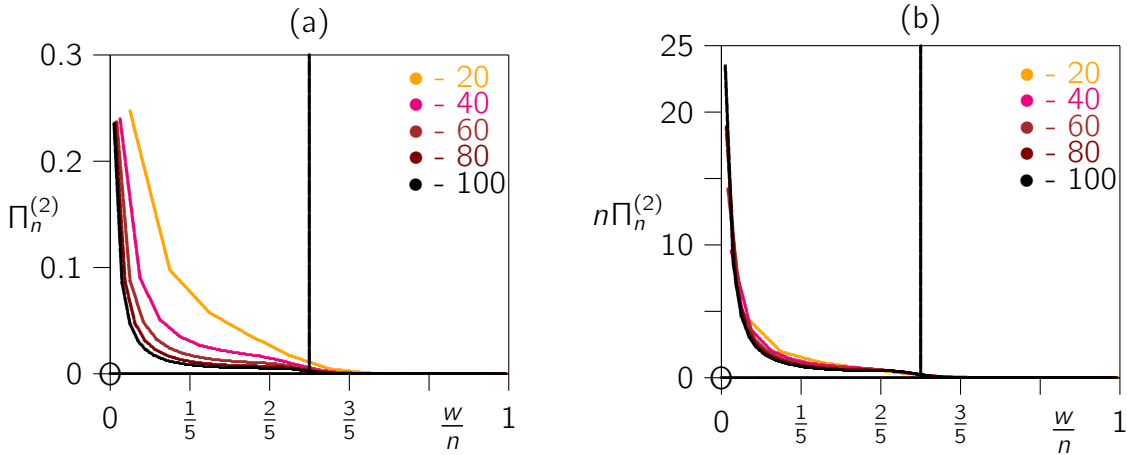


Figure 16: The pressures  $\Pi_n^{(2)}(w)$  as a function of  $w$  with  $a = 1$ . (a) The pressures for  $n$  in  $\{20, 40, 60, 80, 100\}$  as interpolated as a function of  $\frac{w}{n}$ . With increasing  $n$  the pressure decreases monotonically. (b) Since the length of a rescaled edge decreases proportional to  $\frac{1}{n}$  with increasing  $n$ , the pressures in (a) can be rescaled by plotting  $n\Pi_n^{(2)}$  against  $\frac{w}{n}$ . This collapses the data in (a) closer together and suggests an underlying limiting rescaled pressure. Note that the data in these graphs are interpolated on odd values of  $w$ .

edges of length  $\frac{1}{n}$ , a multiplication of  $\Pi_n^{(1)}(w, 0)$  by  $n$  should rescale the pressure curves to compensate; there may even be a limiting (non-zero) pressure curve in the limit as  $n \rightarrow \infty$  in this model. This possibility is explored in figure 15(b), and while there remains some spread in the curves, they do cluster nicely together.

In figure 16(a) the data for the pressure  $\Pi_n^{(2)}(w)$  is interpolated on  $\frac{w}{n}$ . Since the endpoint of the walk is unconstrained in this case, the pressure declines to zero with increasing  $w$  without the presence of a secondary peak (see figure 15(a)). These data can also be rescaled by plotting  $n\Pi_n^{(2)}$  in figure 16(b) against  $\frac{w}{n}$ . This exposes, as in

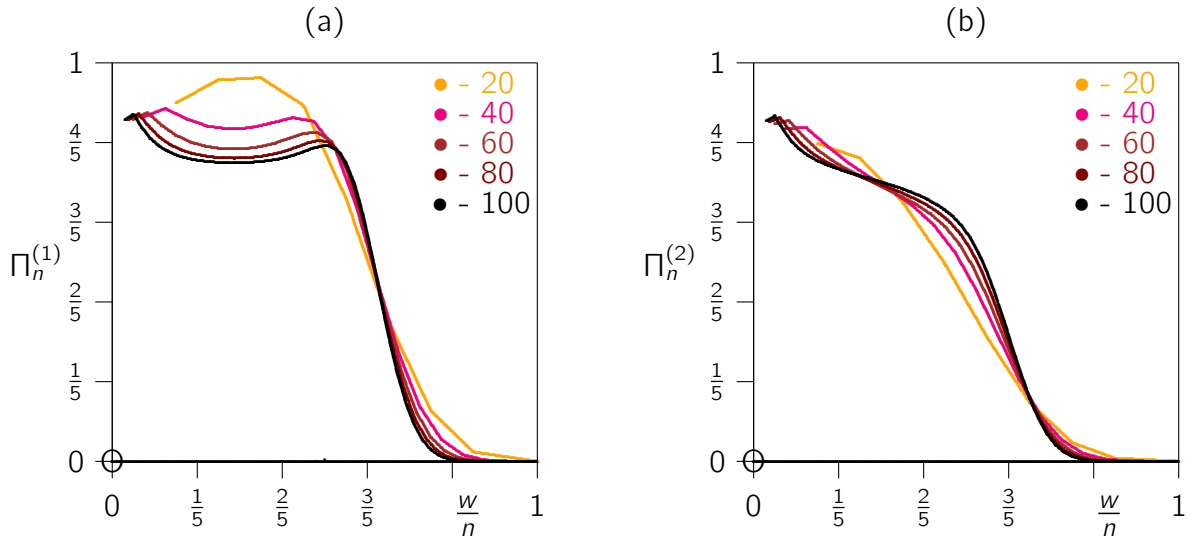


Figure 17: The pressures  $\Pi_n^{(1)}(w, 0)$  (for partially directed walks with endpoint at height  $h = 0$  and with  $a = 2$ ) and  $\Pi_n^{(2)}(w)$  (for partially directed walks with endpoint at any height  $h$  and with  $a = 2$ ) as a function of  $w$ . (a) The pressures for partially directed paths walks (or bargraph paths) with endpoint at height  $h = 0$  for  $n$  in  $\{20, 40, 60, 80, 100\}$  as interpolated as a function of  $\frac{w}{n}$ . For  $w$  less than about  $\frac{1}{2}n$  the pressures are large, and while slowly decreasing, may approach a non-zero constant as  $n \rightarrow \infty$ . For  $w$  large the pressure approaches zero. Note that there is no-rescaling of  $\Pi_n^{(1)}(w, 0)$  by  $n$  in this figure, unlike the graph displayed in figure 15(b). (b) The pressures for walks with endpoint at any height, for  $n$  in  $\{20, 40, 60, 80, 100\}$ , as interpolated as a function of  $\frac{w}{n}$ . These pressures were also not rescaled by  $n$ , unlike the data in figure 16(b). For small values of  $w$  the pressures are large and non-vanishing, but for large values of  $w$  the pressures approach zero. Note that the data in this graphs are interpolated on odd values of  $w$ .

figure 15(b), an apparent limiting pressure curve.

In figure 17 the pressures are displayed for  $a = 2$ ; that is, when the walk is adsorbed onto  $\partial\mathbb{L}_+^2$ . Comparison to the data in figures 15(a) and 16(a) shows that the pressures here are larger, and moreover, for small values of  $w$ , do not decrease markedly with increasing  $n$ . In fact, for values of  $w$  less than about  $\frac{1}{2}n$  both the data for  $\Pi_n^{(1)}$  and  $\Pi_n^{(2)}$  suggest that the pressures converges to a non-zero value as  $n$  becomes very large. For large values of  $w$ , the pressures approach zero.

## 6. Conclusions

In this paper a two dimensional partially directed walk model was used to examine the forces and pressures of a linear polymer near an adsorbing wall. We determined the generating function of the model, and used it to compute the entropic forces it induces between two vertical confining walls, and also to determine the pressure exerted on the adsorbing wall.

Similar lattice models of the entropic forces in polymers have been examined elsewhere. For example, in reference [13] a self-interacting self-avoiding walk model of pulled walks was examined in  $\mathbb{L}^2$  using exact enumeration data. In the constant distance ensemble the force-extension curves were determined for walks below, at, and above the  $\theta$ -temperature. The results (see for example figure 9 in [13]) show that the

force is attractive (pulling the end-points of the walks together) if the distance between the endpoints is a non-zero constant fraction of  $n$  (the length of the walk). This is not surprising, since the natural length scale in this model is  $n^\nu$  (where  $\nu < 1$  is the metric exponent of the self-avoiding walk). Thus, there is no zero force point in this model.

It is possible to prove that there is no zero force point in a model of self-avoiding walks confined to a slit of fixed width  $w$ . This may be done as follows. A *bridge* is a self-avoiding walk from the origin, with first step in the  $x$ -direction, never to return to the  $x = 0$  plane, and with last vertex having maximal  $x$ -coordinate (see, for example, reference [22] for a definition). If a bridge has  $x$ -span equal to  $w$ , then it has *width*  $w$ . If the number of bridges of length  $n$  and width  $w$  is denoted  $\beta_n(w)$ , then the growth constant  $\mu_w$  is known to exist (see, for example, reference [16]), and is given by

$$\log \mu_w = \lim_{n \rightarrow \infty} \frac{1}{n} \log \beta_n(w). \quad (77)$$

The force on the vertical walls is given by the discrete derivative

$$F_w = \log \mu_w - \log \mu_{w-1}. \quad (78)$$

It is known that  $\mu_{w-1} < \mu_w < \mu$ , where  $\mu$  is the growth constant of the self-avoiding walk [16]. This shows that  $F_w > 0$  for all values of  $w$ , and there is no zero force point in this model. Moreover, taking  $w \rightarrow \infty$  shows that  $\lim_{w \rightarrow \infty} F_w = 0$ , since  $\mu_w \rightarrow \mu$  as  $w \rightarrow \infty$  [16].

An alternative model, with length in the horizontal direction scaled by  $n$  is obtained by choosing  $w = \lfloor \alpha n \rfloor$  in the above model. The partition function of this model is defined by  $Z_n(\alpha) = \beta_n(\lfloor \alpha n \rfloor)$ . The (extensive) free energy of this model is given by  $F_n(\alpha) = \log Z_n(\alpha)$ . The microcanonical density conjugate to the width of bridges in this model is defined by the limit

$$P(\alpha) = \lim_{n \rightarrow \infty} (\beta_n(\lfloor \alpha n \rfloor))^{1/n}. \quad (79)$$

It can be shown that this limit exists (see reference [15]), and is a log-concave function of  $\alpha \in [0, 1]$ , and so is differentiable for almost every  $\alpha \in (0, 1)$ .

Define the free energy of *pulled bridges* in the *constant force ensemble* by

$$\mathcal{F}(x) = \lim_{n \rightarrow \infty} \frac{1}{n} \log \sum_{w=0}^n \beta_n(w) x^w \quad (80)$$

where  $x = e^f$  (and  $f$  is the horizontal pulling force on the endpoint of the bridge). This limit can also be shown to exist (see reference [15] for more details). The microcanonical density function  $P(\alpha)$  is related to the Legendre transform of  $\mathcal{F}(x)$ , namely

$$\log P(\alpha) = \inf_{x>0} \{ \mathcal{F}(x) - \alpha \log x \}. \quad (81)$$

It is known that  $\mathcal{F}(x)$  is a convex function of  $\log x$  and that

$$\mathcal{F}(x) \begin{cases} = \log \mu, & \text{if } x \leq 1; \\ > \log \mu, & \text{if } x > 1. \end{cases} \quad (82)$$

For proofs of these facts, see references [1, 20]. This implies that, (1) the right derivative of  $P(\alpha)$  at  $\alpha = 0$  is equal to 0, and (2)  $P(\alpha)$  is strictly decreasing for  $\alpha \in (0, 1]$ .

The limiting force on the vertical walls in this model is given by

$$F_\alpha = \frac{d}{d\alpha} \log P(\alpha). \quad (83)$$

By the properties of  $P(\alpha)$ , this shows that  $F_\alpha$  is a strictly negative force for all values of  $\alpha \in (0, 1)$  (implying that it pulls the vertical walls together). Moreover,  $F_0 = 0$  and  $F_\alpha$  is a (strictly) decreasing function of  $\alpha > 0$ , showing that the magnitude of the pulling force increases as the endpoints of the bridge are taken further apart. That is, there are no zero force points in this model as well.

In contrast to the results for the self-avoiding walk discussed above, our results show that the forces between confining walls may be either attractive (if the endpoints of the walk are far apart), or repulsive (if the endpoints are close together). Generally the strength of the repulsive forces increases if the walk adsorbs on the adsorbing wall, as seen, for example, in figure 11(b).

A particular interesting result is the location of the zero force point in the models. For bargraph paths (when  $h = 0$  and  $a = 1$  in section 3.1.1) this point is located at  $\alpha_c(0) = \frac{1}{2}$ , so that the force vanishes when the horizontal extent of the path is one-half its total length. The location of this point does not move with increasing attraction into the adsorbing line in the desorbed phase, as seen in section 3.1.3, where at the critical point  $a_c$ , the zero force point is still located at  $\alpha = \frac{1}{2}$ . In other words, for all desorbed bargraph paths, the zero force point is located at  $\alpha = \frac{1}{2}$  (this may be verified by using the full expression for the free energy  $F(\alpha, \phi)$  in section 3.1.5 (and by putting  $\phi = 0$  therein).

For values of  $a \geq a_c$  and  $\phi > 0$  the location of the zero force point becomes more interesting. In particular, for  $a = a_c$  the location of this point is a function of  $\phi$  given in equation (55), and approximate locations for the zero force point in the adsorbed phase (where  $a > a_c$ ) are given for  $\phi = 0$  in equations (56) and (57).

We also succeeded in developing an asymptotic formula for the partition function of the partially directed walk in the case that  $a = 1$  and  $h = 0$  (these are bargraph paths). This result was used to verify our results, and it shows excellent agreement.

We examined the pressure of the walk on the adsorbing wall – this is always positive, and is sharply peaked near the origin (where the walk is tethered to the adsorbing wall). Rescaling the pressure (see for example figure 15) shows a secondary peak at the average position of the freely moving endpoint of the walk.

**Acknowledgements:** EJJvR acknowledges financial support from NSERC (Canada) in the form of a Discovery Grant.

## References

- [1] N R Beaton. The critical pulling force for self-avoiding walks. *J Phys A Math Theo*, 48:16FT03, 2015.
- [2] HD Bijsterbosch, VO De Haan, AW De Graaf, M Mellema, FAM Leermakers, MA Cohen Stuart, and AA van Well. Tethered adsorbing chains: Neutron reflectivity and surface pressure of spread diblock copolymer monolayers. *Langmuir*, 11(11):4467–4473, 1995.
- [3] M Bousquet-Mélou and M Mishna. Walks with small steps in the quarter plane. *Contemp Math*, 520:1–40, 2010.
- [4] R Brak, AL Owczarek, and A Rechnitzer. Exact solutions of lattice polymer models. *J Math Chem*, 45:39–57, 2009.

- [5] R Brak, AL Owczarek, A Rechnitzer, and SG Whittington. A directed walk model of a long chain polymer in a slit with attractive walls. *J Phys A: Math Gen*, 38:4309–4325, 2005.
- [6] MA Carignano and I Szleifer. On the structure and pressure of tethered polymer layers in good solvent. *Macromol*, 28(9):3197–3204, 1995.
- [7] MCTP Carvalho and V Privman. Directed walk models of polymers at interfaces. *J Phys A: Math Gen*, 21:L1033–L1037, 1988.
- [8] EA DiMarzio and RJ Rubin. Adsorption of a chain polymer between two plates. *J Chem Phys*, 55:4318–4336, 1971.
- [9] P Flajolet and R Sedgewick. *Analytic Combinatorics*. Cambridge University Press, 2009.
- [10] DP Foster. Exact evaluation of the collapse phase boundary for two-dimensional directed polymers. *J Phys A: Math Gen*, 23:L1135–L1138, 1990.
- [11] F Gassoumov and EJ Janse van Rensburg. The entropic pressure of a lattice polygon. *J Stat Mech: Theo Exp*, 2013(10):P10005, 2013.
- [12] A Gholami, J Wilhelm, and E Frey. Entropic forces generated by grafted semiflexible polymers. *Phys Rev E*, 74(4):041803, 2006.
- [13] A Guttmann, J Jacobsen, I Jensen, and S Kumar. Modeling force-induced bio-polymer unfolding. *J Math Chem*, 1(45):223–237, 2009.
- [14] EJ Janse van Rensburg. The entropic pressure of lattice knots. *J Stat Mech: Theo Exp*, 2014(06):P06017, 2014.
- [15] EJ Janse van Rensburg. *The Statistical Mechanics of Interacting Models of Self-Avoiding Walks, Polygons, Animals and Vesicles*. Oxford University Press, 2015.
- [16] EJ Janse van Rensburg, E Orlandini, and SG Whittington. Self-avoiding walks in a slab: Rigorous results. *J Phys A: Math Gen*, 39:13869–13902, 2006.
- [17] EJ Janse van Rensburg and T Prellberg. The pressure exerted by adsorbing directed lattice paths and staircase polygons. *J Phys A: Math Theo*, 46(11):115202, 2013.
- [18] EJ Janse van Rensburg and A Rechnitzer. Exchange symmetries in Motzkin path and bargraph models of copolymer adsorption. *Elect J Comb*, 9(R20):1, 2002.
- [19] EJ Janse van Rensburg and A Rechnitzer. The compressibility of minimal lattice knots. *J Stat Mech: Theo Exp*, 2012:P05003, 2012.
- [20] EJ Janse van Rensburg and SG Whittington. Self-avoiding walks subject to a force. *J Phys A Math Gen*, 49:11LT01, 2016.
- [21] I Jensen, WG Dantas, CM Marques, and JF Stilck. Pressure exerted by a grafted polymer on the limiting line of a semi-infinite square lattice. *J Phys A: Math Theo*, 46(11):115004, 2013.
- [22] N Madras and G Slade. *The Self-Avoiding Walk*. Birkhäuser, 1993.
- [23] Maplesoft. *Maple 17*. A division of Waterloo Maple Inc., Waterloo, Ontario.
- [24] CM Mate and VJ Novotny. Molecular conformation and disjoining pressure of polymeric liquid films. *J Chem Phys*, 94:8420–8437, 1991.
- [25] G Nägele, B D’Aguanno, and AZ Akcasu. Preface of Proceedings of the Workshop on Colloid Physics held at the University of Konstanz, Germany from 30 November to 2 December 1995. Elsevier, 1997.
- [26] J-A Osborn and T Prellberg. Forcing adsorption of a tethered polymer by pulling. *J Stat Mech: Theo Expr*, 2010(09):P09018, 2010.
- [27] CE Soteros and SG Whittington. Polygons and stars in a slit geometry. *J Phys A: Math Gen*, 21:L857–L861, 1988.
- [28] HNV Temperley. Combinatorial problems suggested by the statistical mechanics of domains and of rubber-like molecules. *Phys Rev*, 103(1):1–16, 1956.
- [29] SG Whittington. A directed-walk model of copolymer adsorption. *J Phys A: Math Gen*, 31:8797–8803, 1998.
- [30] SG Whittington and CE Soteros. Polymers in slabs, slits, and pores. *Israel J Chem*, 31:127–133, 1991.
- [31] SG Whittington and CE Soteros. Uniform branched polymers in confined geometries. *Macromol Rep*, 29(S2):195–199, 1992.